AD-A132 858 AN ACOUSTIC LEVITATION TECHNIQUE FOR THE STUDY OF NONLINEAR OSCILLATIONS O.. (U) MISSISSIPPI UNIV UNIVERSITY PHYSICAL ACOUSTICS RESEARCH GROUP.. 1/1

UNCLASSIFIED D A YOUNG ET AL. 15 AUG 83 PARGUM-2-83 F/G 20/4 NL

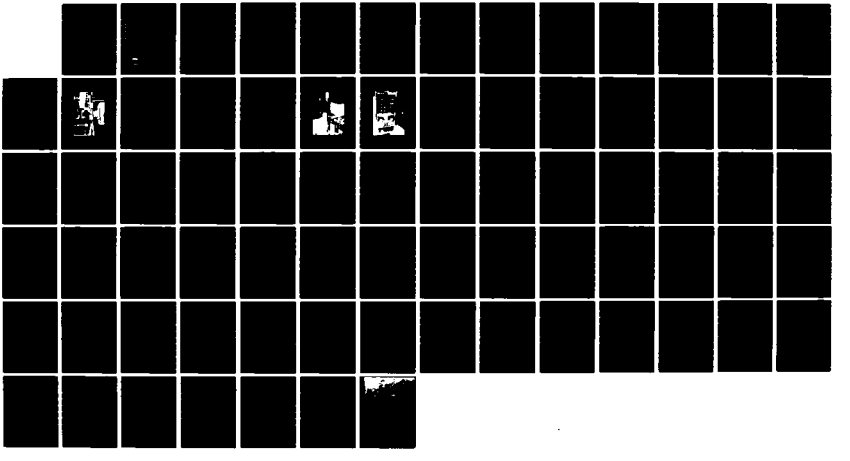

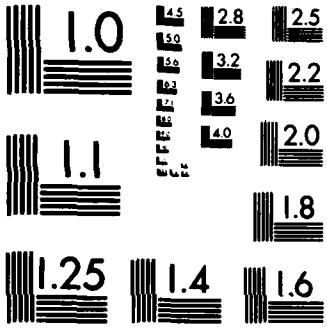

MICROCOPY RESOLUTION TEST CHART
NATIONAL BUREAU OF STANDARDS-1963-A

AN ACOUSTIC LEVITATION TECHNIQUE FOR THE STUDY OF NONLINEAR OSCILLATIONS OF GAS BUBBLES IN LIQUIDS

THE UNIVERSITY OF MISSISSIPPI
PHYSICAL ACOUSTICS RESEARCH GROUP
DEPARTMENT OF PHYSICS AND ASTRONOMY

(12)

Technical Report for
Office of Naval Research
Contract N00014-81-K-0691

AN ACOUSTIC LEVITATION TECHNIQUE FOR THE STUDY OF NONLINEAR OSCILLATIONS OF GAS BUBBLES IN LIQUIDS

by

D. A. Young* and L. A. Crum
Physical Acoustics Research Laboratory
Department of Physics and Astronomy
The University of Mississippi
University, Mississippi 38677

August 15, 1983

*MS Thesis directed by Lawrence A. Crum

Unclassified

SECURITY CLASSIFICATION OF THIS PAGE (When Data Entered)

REPORT DOCUMENTATION PAGE		READ INSTRUCTIONS BEFORE COMPLETING FORM
1. REPORT NUMBER: 2-83	2. GOVT ACCESSION NO.	3. RECIPIENT'S CATALOG NUMBER
4. TITLE (and Subtitle): Nonlinear Gas Bubble Oscillations		5. TYPE OF REPORT & PERIOD COVERED: Technical
		6. PERFORMING ORG. REPORT NUMBER
7. AUTHOR(s): D. A. Young and L. A. Crum		8. CONTRACT OR GRANT NUMBER(s): N00014-81-K-0691
9. PERFORMING ORGANIZATION NAME AND ADDRESS: Physical Acoustics Research Laboratory, Department of Physics, University of Mississippi, Univ., Miss. 38677		10. PROGRAM ELEMENT, PROJECT, TASK AREA & WORK UNIT NUMBERS: NR384-836
11. CONTROLLING OFFICE NAME AND ADDRESS: Office of Naval Research, Physics Division, Code 412, Arlington, VA 22217		12. REPORT DATE: 8-15-83
		13. NUMBER OF PAGES: 67
14. MONITORING AGENCY NAME & ADDRESS (if different from Controlling Office)		15. SECURITY CLASS. (of this report): Unclassified
		15a. DECLASSIFICATION/DOWNGRADING SCHEDULE

16. DISTRIBUTION STATEMENT (of this Report)

Approved for Public Release; distribution unlimited

17. DISTRIBUTION STATEMENT (of the abstract entered in Block 20, if different from Report)

18. SUPPLEMENTARY NOTES

19. KEY WORDS (Continue on reverse side if necessary and identify by block number)

Cavitation
Bubbles
Nonlinear Oscillations

20. ABSTRACT (Continue on reverse side if necessary and identify by block number)

A technique of acoustic levitation was developed for the study of individual gas bubbles in a liquid. Isopropyl alcohol and a mixture of glycerine and water (33-1/3% glycerine by volume) were the two liquids used in this research. Bubbles were levitated near the acoustic pressure antinode of an acoustic wave in the range of 20-22 kHz. Measurements were made of the levitation number as a function of the normalized

DD FORM 1 JAN 73 1473 EDITION OF 1 NOV 65 IS OBSOLETE

S/N 0102-LF-014-6601

UNCLASSIFIED

SECURITY CLASSIFICATION OF THIS PAGE (When Data Entered)

radius of the bubbles. The levitation number is the ratio of the hydrostatic pressure gradient to the acoustic pressure gradient. These values were then compared to a nonlinear theory. Results were very much in agreement except for the region near the n=2 harmonic. An explanation for the discrepancy between theory and experiment appears to lie in the polytropic exponent associated with the gas in the interior of the bubble.

ACKNOWLEDGEMENTS

I would like to express my appreciation to Dr. L.A. Crum for his guidance and instruction during this project, to the Office of Naval Research and the National Science Foundation for the funding which made this project possible, to Charles Herring for his help during data collection and analysis, and to my friend Katherine for her assistance and support during this part of my life.

TABLE OF CONTENTS

Page

LIST OF FIGURES

FIGURE Page

INTRODUCTION

Recently, there has been a revival of interest in the dynamics of a single bubble driven into pulsation by an applied acoustic field. A technique was needed which would allow the close examination of an individual, undistorted bubble. Methods which allow the trapping of a bubble in a sound field by some mechanical constraint do exist, but these techniques distort the bubble and introduce nearby boundaries.

The purpose of this project was to develop a technique to study the nonlinear oscillations of bubbles free from the effects of mechanical constraints. The technique to be described here has been called acoustic levitation. A splendid isolation for the individual bubble, removing it by over 500 bubble diameters from the nearest solid surface can be obtained by this technique. It also allows the individual bubble to be viewed with little difficulty using a small magnification microscope, which in turn enables one to make a precise determination of its position and any changes in that position. Using this technique, the bubble may be accurately positioned to within one-half of its diameter in the sound field.

It was desired that the bubble's size should vary over an order of magnitude for the range of interest in this study, and consequently a method was needed for measuring this range of sizes. Using the acous-

tic levitation technique, the bubble's size can be determined by measuring its terminal velocity as it rises freely through the liquid and applying an appropriate drag law. Accordingly, a wide range of bubble "rise distances" was needed. With this technique, the range of rise distances over which the bubble's size could be determined varied from less than 1 mm to nearly 16 mm, enabling measurements of the bubble radius to be made from about 10 μm to over 200 μm.

Acoustic levitation occurs when an acoustic "radiation-pressure" force is used to balance the gravitational or buoyancy force which tends to force a bubble toward the surface. The bubble can be trapped over a range of positions near a pressure antinode as a result of the balancing of these two forces.

The acoustic levitation technique was essentially invented by Eller,[1] and was developed in great detail for use with liquids by Apfel.[2] Crum[3,4] has refined the technique and used it extensively in the study of gas bubbles in liquids. As an interesting sidelight, the Jet Propulsion Laboratory[5] plans to use acoustic levitation of liquid metals in air in a future space shuttle mission.

By levitating an air bubble near the pressure antinode of the acoustic sound wave, it was possible to observe small changes in its position as a function of radius as the bubble grew or dissolved. These measurements were then used to investigate the nonlinear oscillations of the bubble over a range of sizes. The bubbles were studied in two liquids: isopropyl alcohol, and a mixture of distilled water and glycerine (33-1/3% glycerine by volume). The temperature of the liquid was also

varied from 9° C to 62° C for different cases of interest. Finally, data was also obtained as a function of acoustic pressure amplitude from about 0.05 bars (5 kPa) to 0.25 bars (25 kPa).

EXPERIMENTAL ARRANGEMENT

The nonlinear oscillations of bubbles in isopropyl alcohol and in a mixture of glycerine and water were studied by use of an acoustic levitation technique. A detailed description of the technique will be given in the experimental methods section.

A Hewlett Packard 200 CD, wide-range audio oscillator was used to generate a signal in the kilohertz range. A Tektronix 545B oscilloscope was used to tune the oscillator to that frequency that gave a maximum in the acoustic pressure amplitude measured by a pill transducer on the side of the levitation cell. This relative maximum indicated that one of the stationary wave resonances of the cell was being excited. The signal to the cell was amplified by a Marantz 8B power amplifier before being introduced into two matched hollow cylindrical transducers which were part of the levitation cell. This device consisted of the two cylindrical transducers separated by a hollow glass cylinder. The transducers were 50 mm in height and had a radius of 7.7 cm. The glass cylinder was 48 mm in height and had walls 2.5 mm thick. Its outer diameter was 6.9 cm. These three parts were cemented together with a thin glass bottom which acted as a flexible pressure release diaphram. The top was covered but not sealed. A photograph of the cell is shown in Fig. 1.

The cell held approximately 400 ml of liquid. A small pill transducer was attached to the outer glass wall of the cell to measure

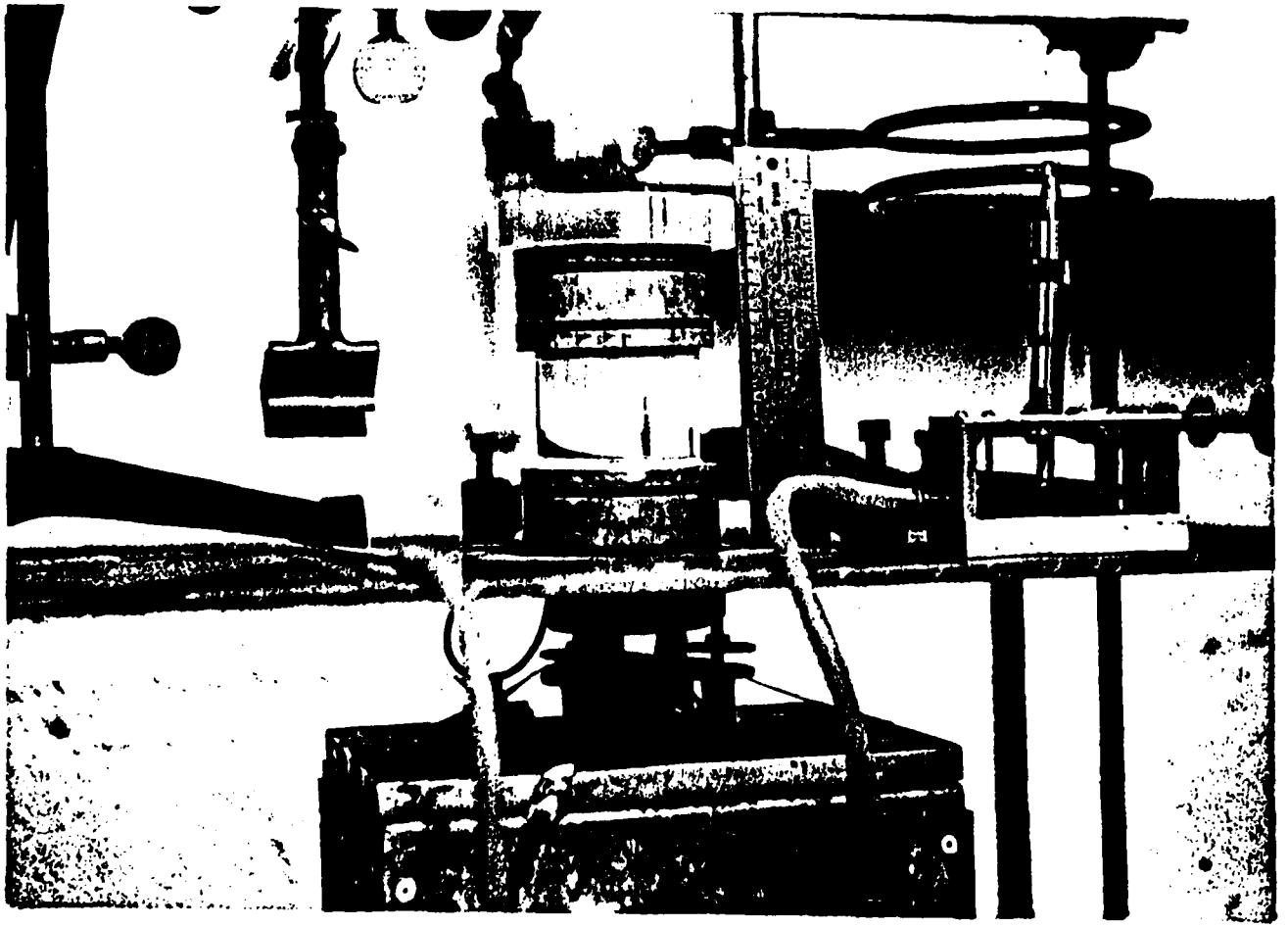

Fig. 1. Photograph of the acoustic levitation cell.

the acoustic pressure amplitude. The signal was amplified by a Hewlett Packard 465A amplifier and its value measured with a Hewlett Packard 3466A multimeter. A Tektronix 545B oscilloscope was used to view the signal of the acoustic pressure generated within the cell, to insure that a pure acoustic mode was generated. A block diagram and sketch of the experimental arrangement is shown in Fig. 2.

A small, calibrated probe hydrophone was used to measure the spatial variation of the stationary acoustic wave along the axis of the cylinder (the acoustic pressure gradient is an important parameter in evaluating the data). This was done prior to data collection. The pill transducer was used in place of the probe hydrophone during data collection. When the bubble radius was to be measured, a toggle switch was used to turn off the audio signal and start an Ortec 875 counter. The switch was held in the "off" position until the bubble was allowed to rise a certain distance while viewed through the cathetometer. The bubble was made visible by the use of a Bausch and Lomb light source which was positioned above the cell and directed so that light would scatter off the bubble. When the switch was returned to the "on" position, the bubble returned to its stable position near the pressure antinode.

The cell was isolated from the room environment by use of an outer container, a temperature control cylinder, which fit around the cell and its leveling support. A Polyscience Polytemp 90 temperature control system was used to pump antifreeze through this cylinder, maintaining a constant temperature in the cell. The temperature of the liquid in the

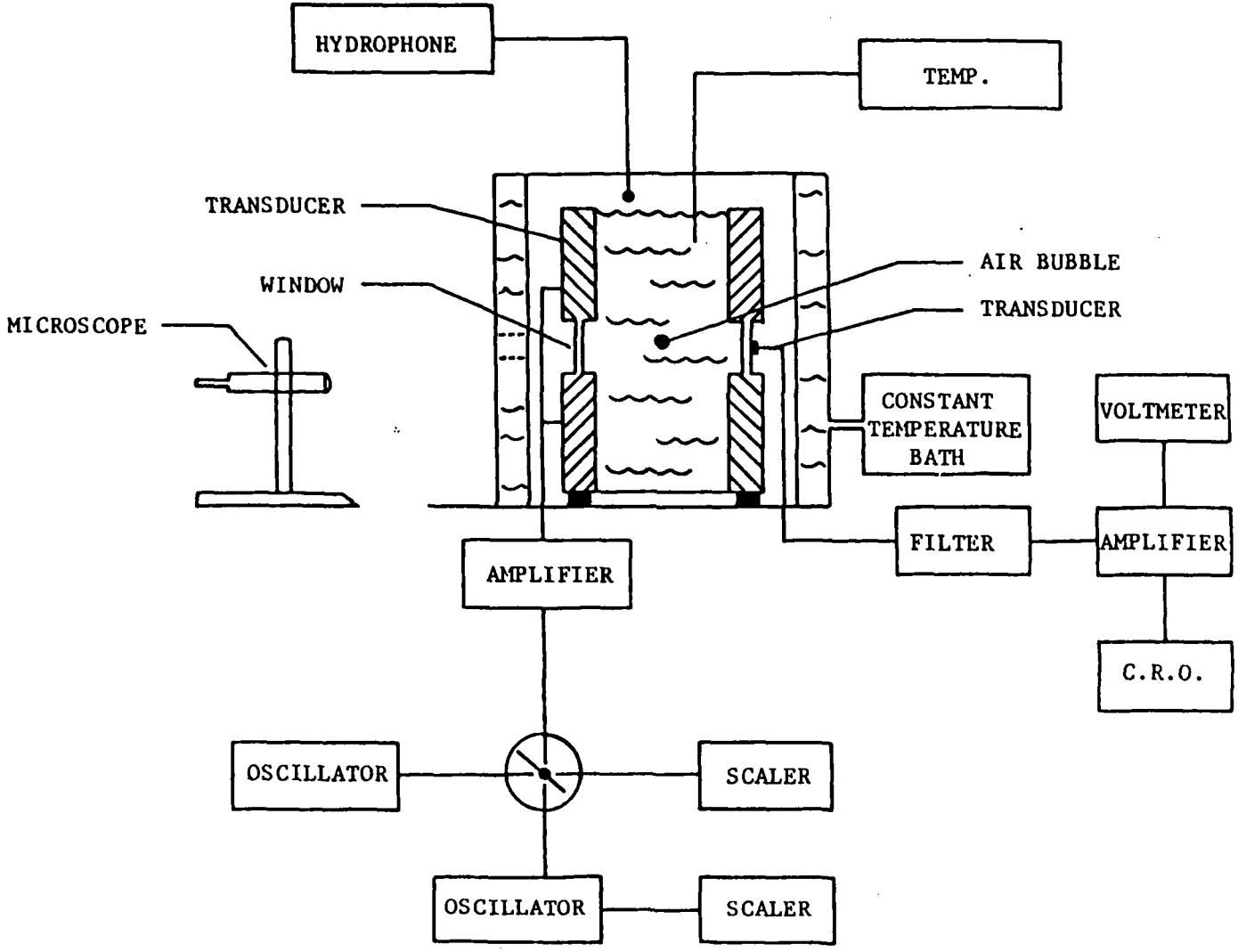

Fig. 2. Block diagram and sketch of the experimental arrangement.

cell was measured by the insertion of a standard thermometer into the liquid through a hole in the cell's cover. Photographs of this system are shown in Fig. 3 and Fig. 4. Fig. 3 shows the cell isolation chamber, the cathetometer used to view the bubble, and the illuminator used to enhance the visibility of the bubble. Fig. 4 shows some of the electronic apparatus used.

Standard methods to adjust the gas content of the liquid were used. An aspirator or a vacuum pump was used to reduce the dissolved gas content of the liquid when needed. The cell was set on a marble slab and on a stand with adjustable legs that enabled it to be leveled. The stand at the base of the cell was surrounded by lead shot, between the temperature control container and the cell's base. The level of liquid was monitored periodically in order to maintain a sound field that did not change with time.

Because dirt particles present in water could (and often would) collect on the surface of the gas bubble, it was necessary to filter the water before using. The glycerine and isopropyl alcohol were clean enough to be used without treatment. Batches of the glycerine/water mixture were made up in large quantities and replacements taken from this large supply so that liquid-property consistency was maintained over several runs.

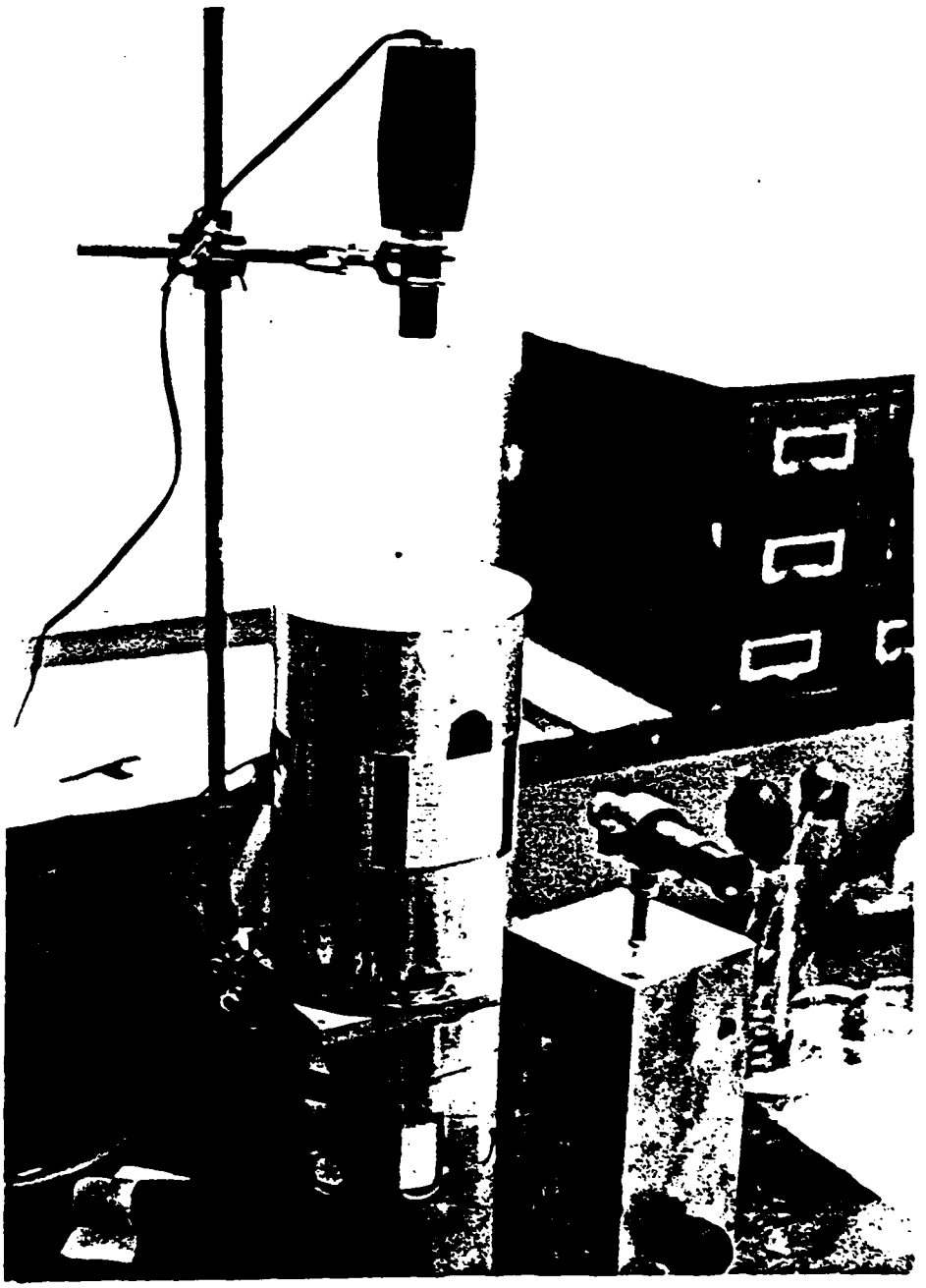

Fig. 3. Photograph of the experimental apparatus (A).

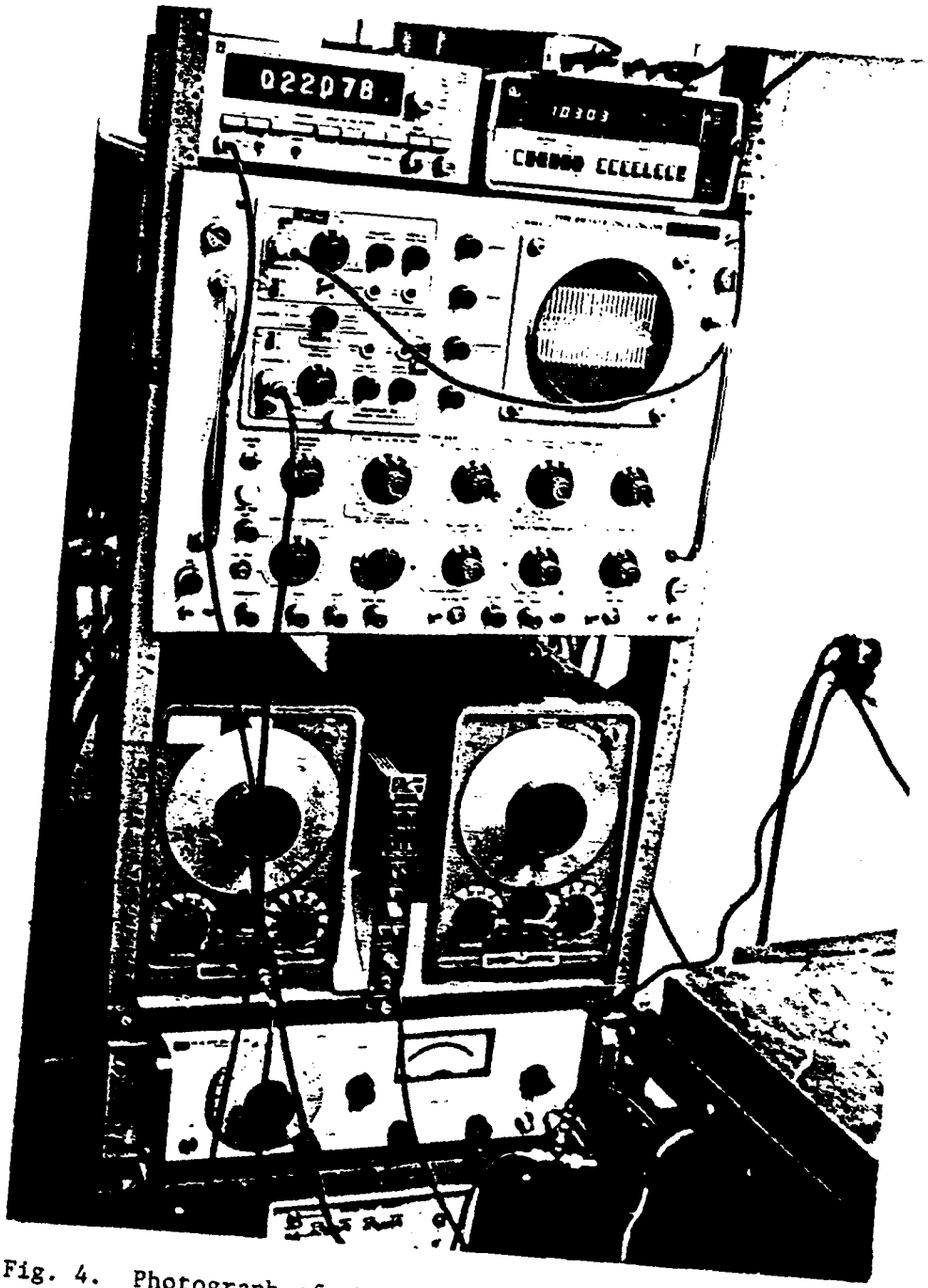

Fig. 4. Photograph of the experimental apparatus (B).

EXPERIMENTAL PROCEDURE

To collect a typical set of data for the analysis of the nonlinear oscillations of a bubble, there were several steps to follow. A mixture of liquid was first prepared and if necessary filtered to remove impurities. The liquid's level was selected so that the pressure antinode for a frequency near 22 kHz was underneath the transparent glass cylinder. If the liquid level was too high or too low, the bubble would assume an equilibrium position that permitted only a limited length of view as it rose during the measurement of its radius. The level of the liquid was adjusted and the correct frequency for that level was determined for each of the different liquids used. However, once the level was determined, a small measuring device was constructed that permitted the level to be repeated after liquid replacement.

Some data was taken as a function of temperature; in these cases, the liquid was brought to the desired temperature before it was introduced into the cell and the temperature control system was used to maintain that temperature. When the temperatures were relatively high (50° C) or low (10° C), there was great difficulty in collecting data. Convection currents would often be present and would affect the balance of forces on the bubble, moving it in a horizontal or vertical direction. Even when data was taken near room temperature (20° C), the temperature control system was used to help avoid any changes in temperature of the liquid over a data collection period. The temperature also affected

the amount of dissolved gas in the liquid. If the liquid had an excess of gas, bubbles would grow at a much more rapid rate than was desired. At other times, the liquid would have such a low level of gas that bubbles were hard to introduce and when one was levitated, it would quickly dissolve. The requirement that the dissolved gas concentration be at a particular value would necessitate the use of one of various systems constructed to change the liquid's gas content, which in turn would affect the temperature, which would affect the gas content, etc. In general, obtaining the optimal liquid conditions for data acquisition was one of many hours of painstaking trial and error adjustments. Another effect of the temperature variation was that, at high temperatures, there was some evaporation which caused the surface to change after a few hours, so data had to be collected and levels adjusted as quickly as possible.

Once the gas content was close to a level which would allow the slow growth or dissolution of the bubble, the frequency was constantly monitored to insure that it was at resonance for the particular standing wave mode throughout the data collection period.

Bubbles were introduced in various manners. One method consisted of increasing the pressure until stable cavitation produced a small bubble. On occasion, a hypodermic needle was used. The introduction of objects into the liquid required care to avoid disturbing the fluid and changing its level. Once a bubble was levitated, care was taken to insure that only one bubble was present. At times, several bubbles could be levitated near the antinode and they would then combine into a

larger bubble due to the secondary or mutual Bjerknes Force.[6] Also, bubbles would appear on the sides of the cell or at the bottom or near other antinodes.

With the individual bubble levitated in the stable liquid, it was then necessary to collect data as the size of the bubble changed. It was found that a large bubble, near the resonance radius, would slowly dissolve if the gas content was slightly less than saturation. A bubble which was small would grow slowly to resonance size through rectified diffusion if the liquid had the correct gas concentration. When the gas conditions were properly set, it became possible to obtain a bubble of any desired size, and data could be collected over a complete range of sizes. The initial size of the bubble selected was determined by visual observation, requiring some experience, but a nomogram showing rise-times over a unit distance for bubbles of various sizes was also used.

With the frequency of the standing wave and the temperature of the liquid known and with a bubble of acceptable size levitated in the liquid, a data set was taken. The location of the bubble was recorded by using the fiducial lines in the cathetometer. The bubble was centered on one of the fiducial lines, usually 1, and a reading was taken from the cathetometer scale, giving the position of the bubble in the sound field. The sound field was then turned off with a toggle switch, allowing the bubble to move toward the surface. The switch also started a timer which measured the time that the sound was off. As viewed through the microscope, the bubble was allowed to move past a number of fiducial

lines before the sound was turned on again to return the bubble back to a position near the antinode. The distance the bubble was allowed to move was determined by various considerations but usually the size of the bubble was the most important. A large bubble would move more rapidly to the surface so a long distance was required in order to reduce errors in the rise-time measurement; a rise-time of 1.5 seconds was usually the minimum value selected. The position of the bubble and the time it took to move a number of fiducial lines were recorded, as well as the voltage, i.e., the acoustic pressure amplitude as measured by the pill transducer. In most data sets, the acoustic pressure was held constant and adjustments were made during data collection only to maintain this voltage.

These steps were repeated for the bubble as its size changed. An attempt was made to obtain measurements of the bubble radius over the range from 10% or 80% of the resonance radius. These measurements were made on a single bubble whenever possible. A set of approximately 10 data points was also made at various voltages for small bubble sizes in order to obtain a calibration curve for each individual data set.

Before the data could be analysed with the computer program, certain physical parameters of the liquid and gas system were needed. Most of the information could be found in references (7) through (11), but for various temperatures of the glycerine/water mixture, the viscosity had to be measured. This was done using as Ostwald Viscometer[12] to measure the time it took the mixture to flow through a given distance in the tube and comparing this to the flow time of a liquid whose viscosity

was known. These viscosity measurements were made for the range of temperatures considered. Other constants used in the data analysis included the liquid's sound speed, its surface tension, and its density. A graph of these values over a range of temperatures is shown in Fig. 5 for isopropyl alcohol, and Fig. 6 for the glycerine/water mixture.

Also required in the data analysis was the ratio of specific heats of the gas, its molecular weight, and its thermal conductivity. The resonance radius for bubbles in the particular liquid was calculated by another computer program as a function of some of the various physical parameters. Various constants were used that related to the levitation cell, such as the wavelength of the sound, and conversion factors to relate the position of the bubble in the sound field to the cathetometer reading and the fiducial lines to standard units of length. These values were obtained during a calibration run.

When all this data (the 17 constants and the measurements from a data set) were gathered, they were entered into a computer program for analysis. From this program, listed in Appendix A as Program 1, the following parameters of interest were obtained: a levitation number (essentially, the ratio of the hydrostatic pressure gradient to the acoustic pressure gradient), the radius of the bubble for each data point entered, the polytropic exponent of the gas contained within the bubble, the acoustic pressure amplitude, and the bubble damping. These parameters can then be compared with theory to test our knowledge of bubble dynamics.

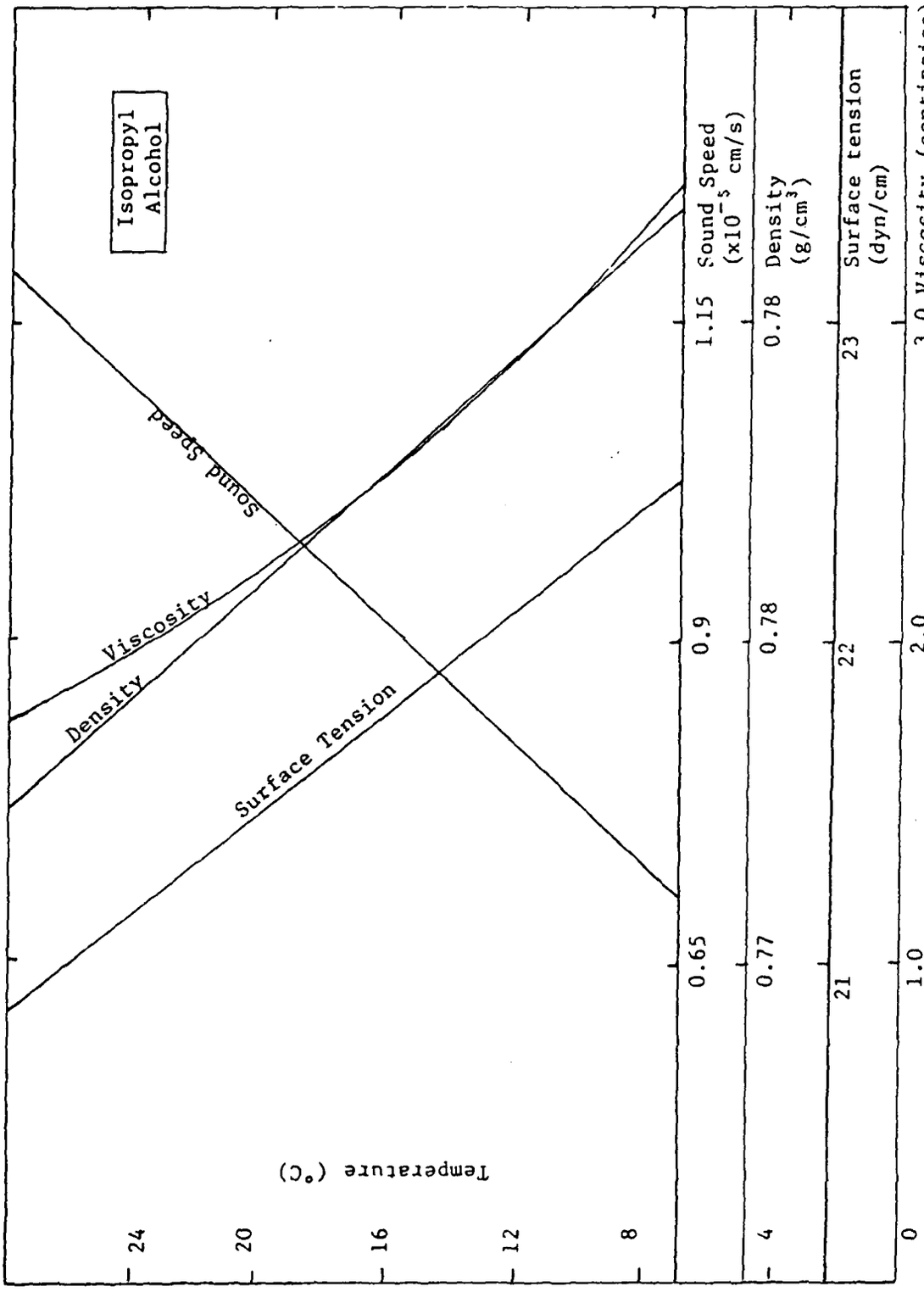

Fig. 5. Variation of viscosity, sound speed, density, and surface tension with temperature for isopropyl alcohol.

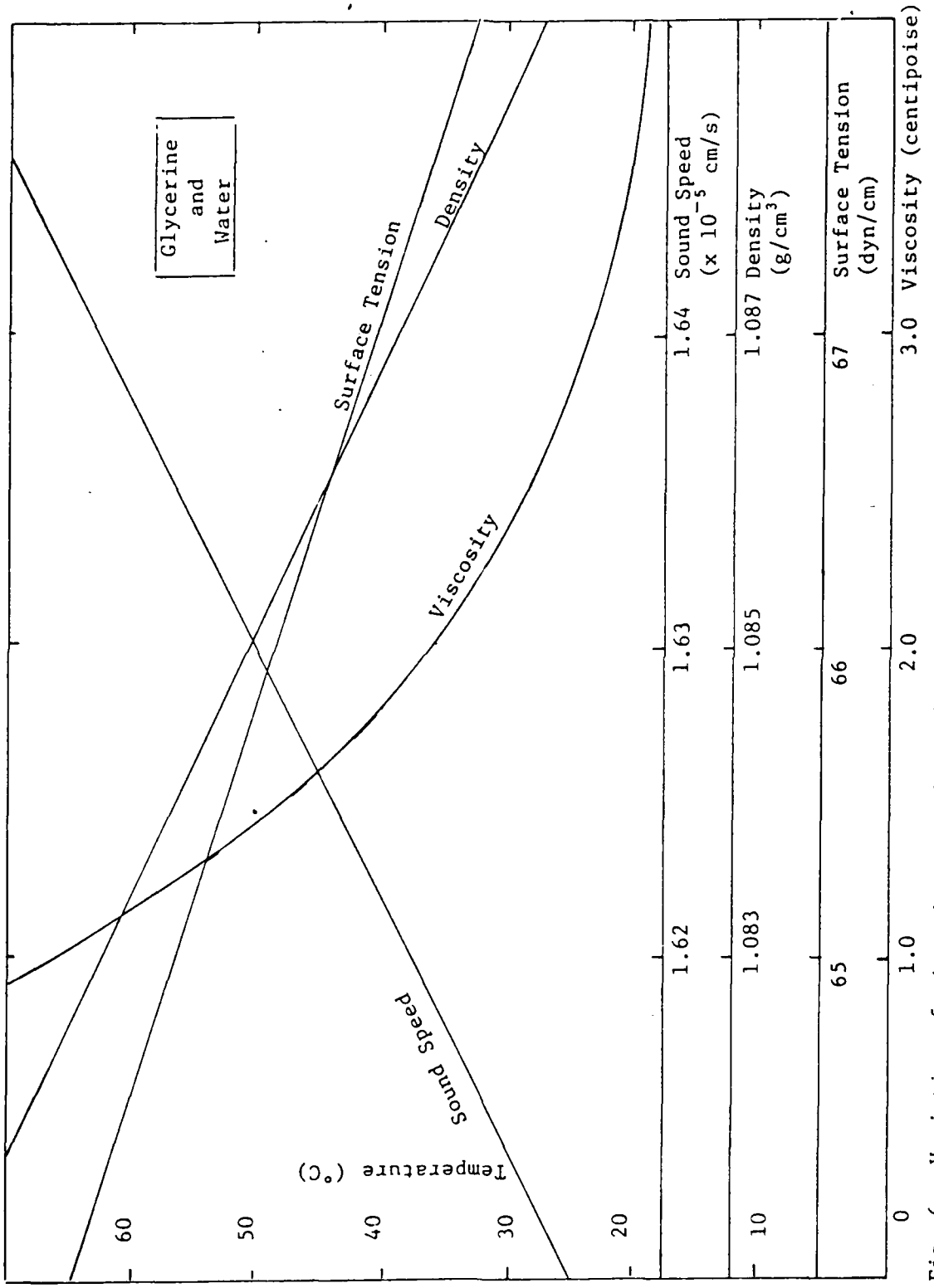

Fig. 6. Variation of viscosity, sound speed, density, and surface tension with temperature for glycerine/water mixture.

THEORY

In this section, the theory relating to the study of the nonlinear oscillations of bubbles by acoustic levitation will be explained briefly. Since this is not a major portion of the study, the reader is referred to previously published articles[6,13] and the computer programs in Appendix A-Poly 5 (Program 1), and Appendix B-CNSTNT (Program 2), which were used to analyze the data. Poly 5 was used to obtain values for levitation number as well as other information already mentioned, while CNSTNT was used to compute values of the theoretical levitation number based on a nonlinear theory. Comparisons of theory and experiment will be made in the data analysis section.

The primary Bjerknes Force, which is the force used to levitate the bubble near the pressure antinode, is given by

$$\vec{F}_A(\vec{r},t) = - \langle V(t) \nabla P(\vec{r},t) \rangle, \tag{1}$$

where the brackets on the right hand side of Eq. (1) mean time average, $V(t)$ is the instantaneous volume of the bubble and $P(\vec{r},t)$ is the time- and space-varying pressure field which can be approximated along the axis of the cell by

$$P(\vec{r},t) = P_\infty - P_A(z)\cos\Omega t. \tag{2}$$

Here P_∞ is the ambient pressure, Ω is the angular frequency of the sound field and $P_A(z)$ is the space-dependent amplitude of the stationary wave, with z being the coordinate measured vertically along the axis of the levitation cell.

When the bubble is spherical with an equilibrium radius of R_0 and an instantaneous radius of R(t), the magnitude of the acoustic force $\vec{F}_A$ may be obtained by substituting Eq. (2) into Eq. (1). This gives

$$F_A = \tfrac{4}{3}\pi R_0^3 |\nabla P_A| \langle [R(t)/R_0]^3 \cos\Omega t \rangle .$$

If the bubble is maintained at a fixed position, the magnitude of the force is balanced by an average gravitational force of magnitude

$$F_B = \tfrac{4}{3}\pi R_0^3 \rho g \langle [R(t)/R_0]^3 \rangle ,$$

where the liquid's density is given by ρ and g is the acceleration due to gravity. This force is a buoyancy force. Equating these two forces yields the following expression:

$$\frac{\langle (R/R_0)^3 \cos\Omega t \rangle}{\langle (R/R_0)^3 \rangle} = \frac{\rho g}{|\nabla P_A|} , \tag{3}$$

with $|\nabla P_A|$ being evaluated at the position in the field where the bubble is being levitated. The right-hand side of Eq. (3) is the ratio of the hydrostatic pressure gradient to the acoustic pressure gradient which is called the levitation number,

$$L_e = \frac{\rho g}{|\nabla P_A|} .$$

If the levitation number is large, it implies that only a small acoustic pressure gradient is needed to levitate a bubble. This implies that the acoustic force is very efficient in stabilizing the bubble against gravity. A small levitation number implies the opposite. In this study, the levitation number is measured experimentally and the left-hand side of Eq. (3) is computed theoretically. This indicates that the results to be shown in the next section can be considered as

comparisons between theoretical and experimental values of the levitation number.

The time-varying radius of the bubble is expressed by the Rayleigh-Plesset equation

$$\rho(R\ddot{R}+\frac{3}{2}\dot{R}^2) = P_i - (P_\infty - P_A\cos\Omega t) - 2\sigma/R - 4\mu\dot{R}/R, \qquad (4)$$

where the surface tension is given by σ, the liquid viscosity by μ, and the instantaneous pressure acting on the gas side of the bubble interface is given by P_i. P_i must be determined by solving the conservation equation relating the gas and the liquid phase. In the case of linear oscillations, the result of these calculations are summarized by stating that the thermal processes result in a pressure-volume relationship of the polytropic type,

$$P_i = P_0(R_0/R)^{3\kappa},$$

where $P_\infty + 2\sigma/R_0$ is the internal pressure of the bubble at equilibrium and κ is the polytropic exponent. It has been shown[14-16] that the thermal processes contribute a dissipation mechanism which can be represented by modifying the value of the liquid viscosity. The acoustic radiation from the bubble also contributes to dissipation, and this effect can also be accounted for by modifying the value of the viscosity.[16] A description of these thermal processes using a polytropic exponent has been experimentally verified[17] for small amplitude oscillations, but an extension of these results for the case of large-amplitude, nonlinear oscillations has never been attempted. Since the nonlinear oscillations are of concern in this study, it is necessary to use the

linear results for κ, and to use the "effective" liquid viscosity, although Eq. (4) will be treated nonlinearly,

For radial pulsations of moderate amplitude, an approximate solution of Eq. (4) can be obtained by using

$$R = R_0[1 + x(t)],$$

and performing a power series expansion of x.[18] For the linear case, the lowest-order approximation to the exact solution can be obtained by retaining only terms which are linear in x and their derivatives. This yields

$$x = \xi\cos(\omega\tau+\delta)/[(\omega^2-\omega_0^2)^2+4b^2\omega^2]^{\frac{1}{2}} ,$$

using the following terminology

$$\tau = (P_0/\rho)^{\frac{1}{2}}\, t/R_0,\ w = 2\sigma/R_0P_0,$$

$$b = 2\mu/R_0(\rho P_0)^{\frac{1}{2}},\ \eta = P_A/P_\infty,$$

$$\xi = (1-w)\eta,\ \omega = R_0\Omega(\rho/P_0)^{\frac{1}{2}},$$

$$\omega_0^2 = 3\kappa-w,\ \delta = \tan^{-1}[2b\omega/(\omega^2-\omega_0^2)].$$

The nondimensional resonance frequency of the bubble is given by ω_0 and when it is converted to dimensional form, it yields the expression

$$\Omega_0 = (1/R_0\rho^{\frac{1}{2}})[3\kappa P_\infty + (3\kappa-1)(\sigma/R_0)]^{\frac{1}{2}}. \qquad (5)$$

The effect of the surface tension's contribution is negligible and κ depends only weakly on R_0 for the range of radius values considered; this implies that $R_0\Omega_0$ is approximately a constant.

If a resonance radius (R_{Res}) is defined by

$$\Omega = (1/R_{Res}\rho^{\frac{1}{2}})[3\kappa P_\infty + (3\kappa-1)(\sigma/R_{Res})]^{\frac{1}{2}} \qquad (6)$$

then $\Omega/\Omega_0 \cong R/R_{Res}$. This implies that for fixed sound frequency (Ω), the ratio Ω/Ω_0 can be varied by changing the radius of the bubble. In the

figures used, the levitation number is compared to R/R_{Res} rather than to Ω/Ω_0 since experimental measurements were made in terms of variable radius rather than variable frequency.

To first order in x, the time averages in Eq. (3) are $\langle(R/R_0)^3 \cos\Omega t\rangle \cong 3\langle x\cos\Omega t\rangle$, and $\langle(R/R_0)^3\rangle \cong 1$. Thus,

$$L_e = \tfrac{3}{2}\,\xi B \cos\delta, \tag{7}$$

where

$$B = [(\omega^2-\omega_0{}^2)^2 + 4b^2\omega^2]^{-\frac{1}{2}}.$$

When the damping is small and the bubble radii are considerably lower than the resonance radius, Eq. (7) becomes

$$L_e \cong (\tfrac{3}{2})\,\frac{1-w}{3\kappa-w}\,\left(\frac{P_A}{P_\infty}\right). \tag{8}$$

In this study for the range of bubble radii investigated, w is very small ($w_{Res} \cong 10^{-2}$) and κ, the polytropic exponent, only weakly depends on R_0. This indicates that the levitation number is only weakly dependent on the bubble radius when R_0 is much smaller than R_{Res}. It has been shown [13] that if the bubble is driven at an amplitude and frequency such that nonlinear effects are significant, the levitation number has an important and measurable dependence on R_0.

Harmonic and subharmonic resonances typical of nonlinear oscillations appear if higher-order terms are used in the solution of Eq. (4). The solution $x(\tau)$ in the harmonic and subharmonic regions allows the explicit calculation of the time averages in Eq. (3). By retaining only terms capable of giving nonzero contributions in the various harmonic resonance regions and keeping a second-order accuracy, the denominator of the left-hand side of Eq. (3) can be taken to be simply 1.0.

For the n = 2 harmonic resonance region, when $\omega \cong \omega_0/2$, the levitation number contains the linear part $\frac{3}{2}\xi B\cos\delta$ plus other terms that are dependent upon the amplitude and phase of the resonant component. At the n = 3 harmonic resonance region, where $\omega \cong \omega_0/3$ it is found that Eq. (3) reduces to the same form found for the linear approximation $\frac{3}{2}\xi B\cos\delta$. For the main resonance n = 1, $\omega = \omega_0$, an expression for the L_e is found in the form of

$$L_e = \frac{3}{2} A_1 \cos\phi_1, \tag{9}$$

where A_1 is the amplitude and ϕ_1 is the phase.

Thus, in general, the levitaion number can be expressed as a linear term plus contributions that apply within individual resonance regions that add additional terms to the linear portion of the theory. These harmonic resonance contributions are extremely complex and won't be given explicitly here, although the theoretical curves shown on the graphs contain an evaluation of both the linear and the nonlinear effects.

To evaluate some of the equations used in the study of the nonlinear oscillations which occur as the bubble changes size, it is necessary to have expressions for the polytropic exponent and the damping constant. The results of the linear theory for these quantities as shown by Eller[14] were used. It has been shown[17] that under normal conditions, measurements of the polytropic exponent for a variety of gases and ranges of bubble sizes agree quite well with the analytical predictions.

The total damping constant b is the sum of the three principal contributions, i.e., viscous, radiation, and thermal. Thus,

$$b = b_v + b_r + b_t \tag{10}$$

where

$$b_v = 2\mu/(\rho P_0)^{\frac{1}{2}} R_0,$$

$$b_r = \tfrac{1}{2}(\rho/P_0)^{\frac{1}{2}}(\Omega^2 R_0^2/c),$$

$$b_t = (\Omega_0^2 R_0/2\Omega)(\rho/P_0)^{\frac{1}{2}} d_t,$$

and

$$d_t = \frac{3(\gamma-1)[X(\sinh X + \sin X) - 2(\cosh X - \cos X)]}{X^2(\cosh X - \cos X) + 3(\gamma-1)X(\sinh X - \sin X)},$$

where c is the sound speed in the liquid, and γ is the ratio of specific heats of the gas contained within the bubble. Also $X = R_0(2\Omega/D_1)^{\frac{1}{2}}$ where D_1 is the thermal diffusivity of the gas defined as $D_1 = K_1/\rho_1 C_{p_1}$, K_1 is its specific heat at constant pressure. The polytropic exponent κ is given by

$$\kappa = \gamma(1 + d_t^2)^{-1}\left[1 + \frac{3(\gamma-1)}{X}\left(\frac{\sinh X - \sin X}{\cosh X - \cos X}\right)\right]^{-1}.$$

These terms are also contained in the computer program used to evaluate the theory.

RESULTS AND DISCUSSION

In this section, the major aspect of this work is examined. The experimental measurements of the bubble's position in the sound field, its "rise-time", and the voltage measured by the external pill transducer are used to obtain values of the levitation number as a function of a radius parameter for various acoustic pressure amplitudes. These values, which were calculated using the computer program in Appendix A, show a variation of the levitation number over a range of normalized bubble radii for both linear and nonlinear oscillations. The normalized radius is the value of the bubble's radius divided by the resonance radius for the given conditions.

Many data sets were taken; shown here are some representative examples at a frequency near 22 kHz. All data presented here were taken with constant values of the acoustic pressure amplitude and the temperature (for a given data set), and these both were then varied over a wide range. Some representative data are shown in Fig. 7 in which the temperature was 35° C and the acoustic pressure amplitude was 0.16 bars. The symbols are experimental points; the dashed and solid lines represent the prediction of the linear and nonlinear theories respectively.

For bubbles less than 40% of the resonance radius, the levitation number is nearly a constant. These points agree very well with theory. Since agreement of small bubble radii with theory was consistently good, these small bubbles were used in each data set to calibrate the sound field within the levitation cell in terms of the voltages measured by

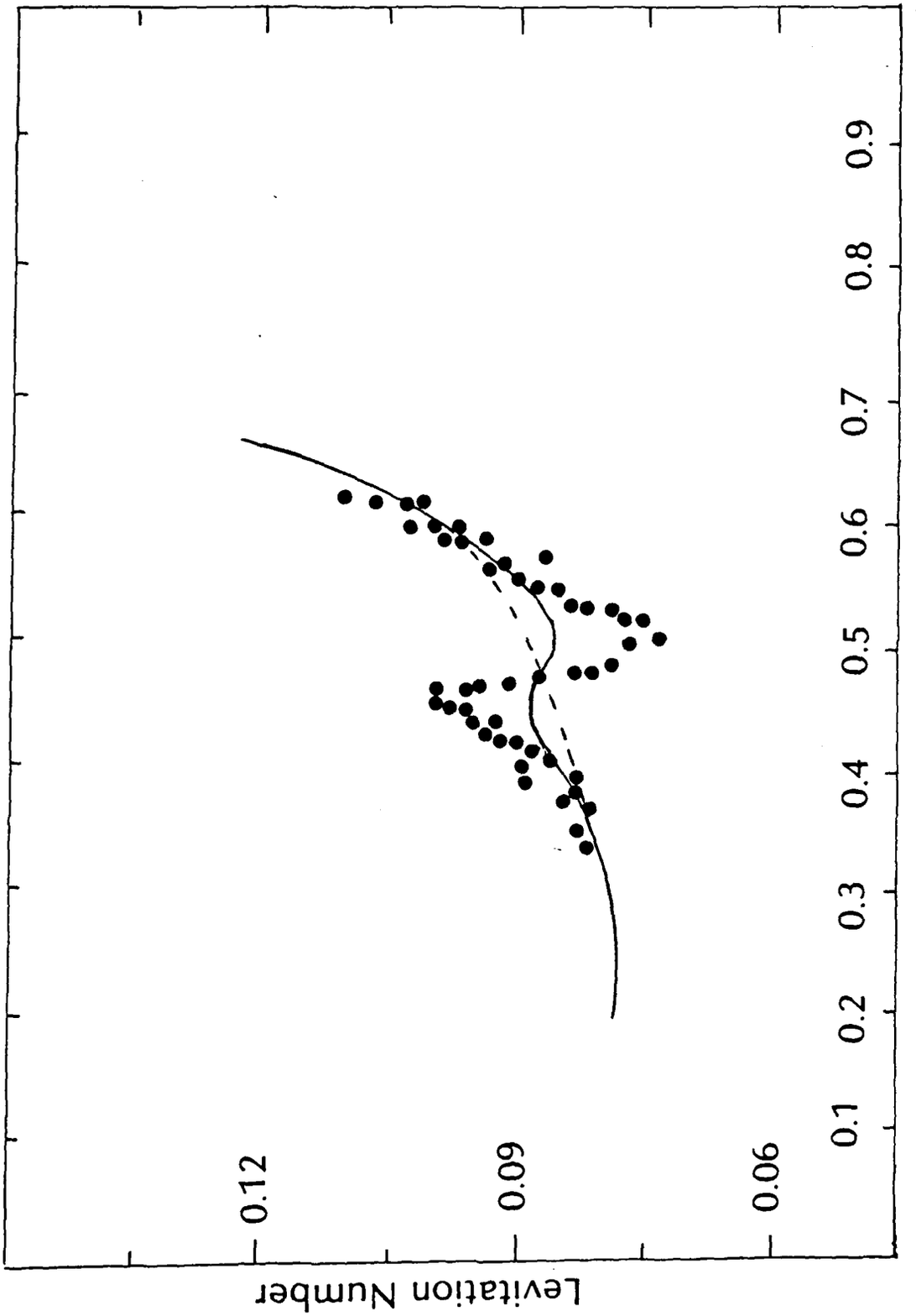

Fig. 7. Variation of levitation number with normalized bubble radius for glycerine/water mixture at 35°C.

the pill transducer. This section of the graph agrees well with theory because the bubbles are just oscillating linearly and the linear theory coincides with the nonlinear theory in this region. In the area from 40% to 55% of resonance radius, the bubbles clearly go into nonlinear oscillations as indicated by the rapid increase, then decrease of the levitation number. The acoustic pressure amplitude for this data is approximately 0.16 bars and the levitation number varies from about 0.08 for small bubbles to about 0.10 for bubbles near harmonic resonance. Bubbles with a normalized radius greater than 0.55 again yield levitation numbers in close agreement with theory.

Fig. 8 shows data using the glycerine/water mixture at 36° C. The acoustic pressure amplitude was 0.19 bars for this case. This higher pressure indicates the relationship between the levitation number and acoustic pressure amplitude when compared with Fig. 7. As the acoustic pressure amplitude increased, so does the levitation number. The match with theory for small and large bubble radii is still apparent, as well as the rapid change in levitation number (up to about 0.11) near harmonic resonance.

Fig. 9 shows data taken at 39° C for glycerine/water. The acoustic pressure amplitude was 0.17 bars and the levitation number for small bubbles in linear oscillations is almost constant at about 0.08. This result is consistent with the two previous figures. The large bubbles with a normalized radius greater than 0.55 also lie along the solid line.

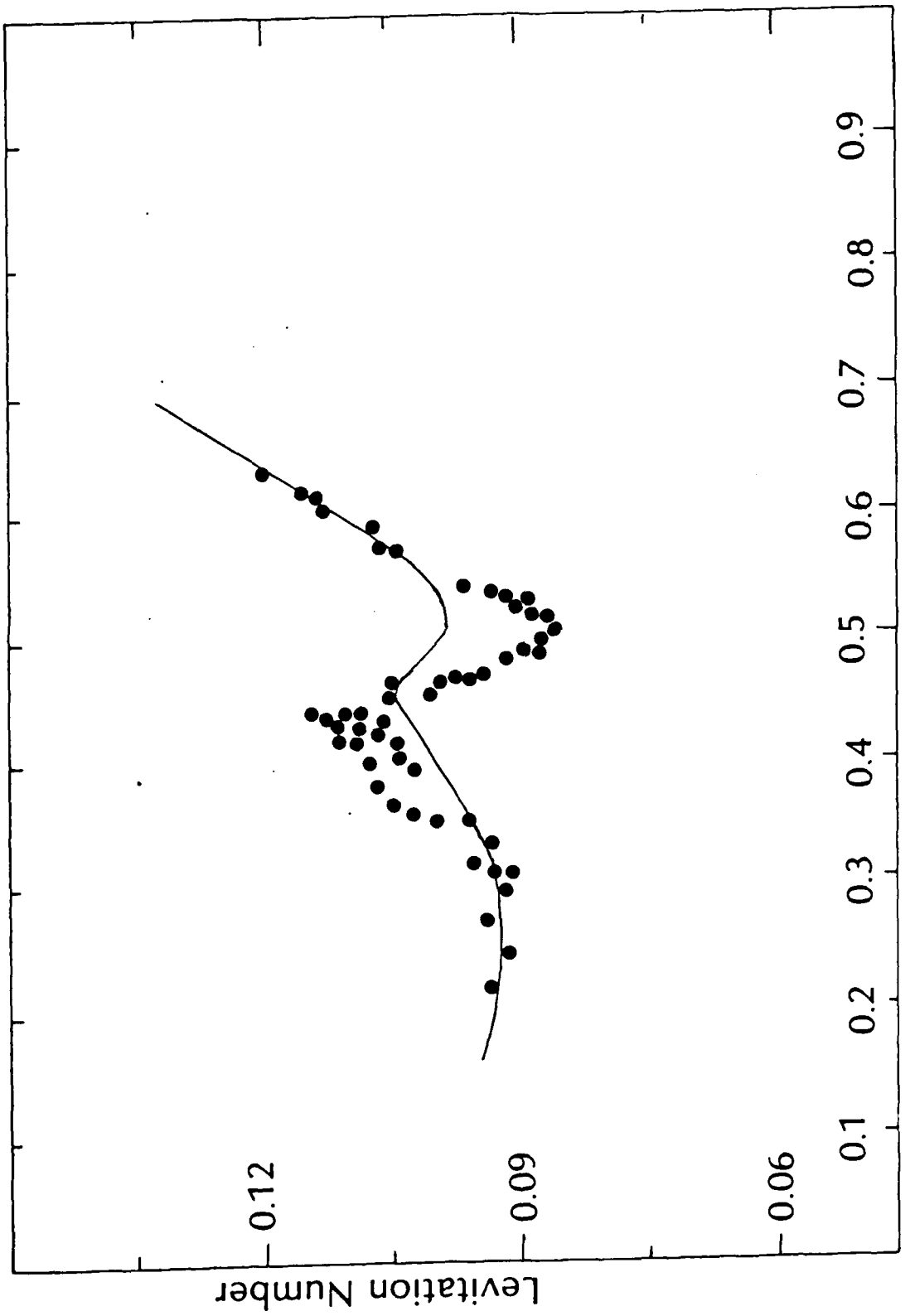

Fig. 8. Variation of levitation number with normalized bubble radius for glycerine/water mixture at 36°C.

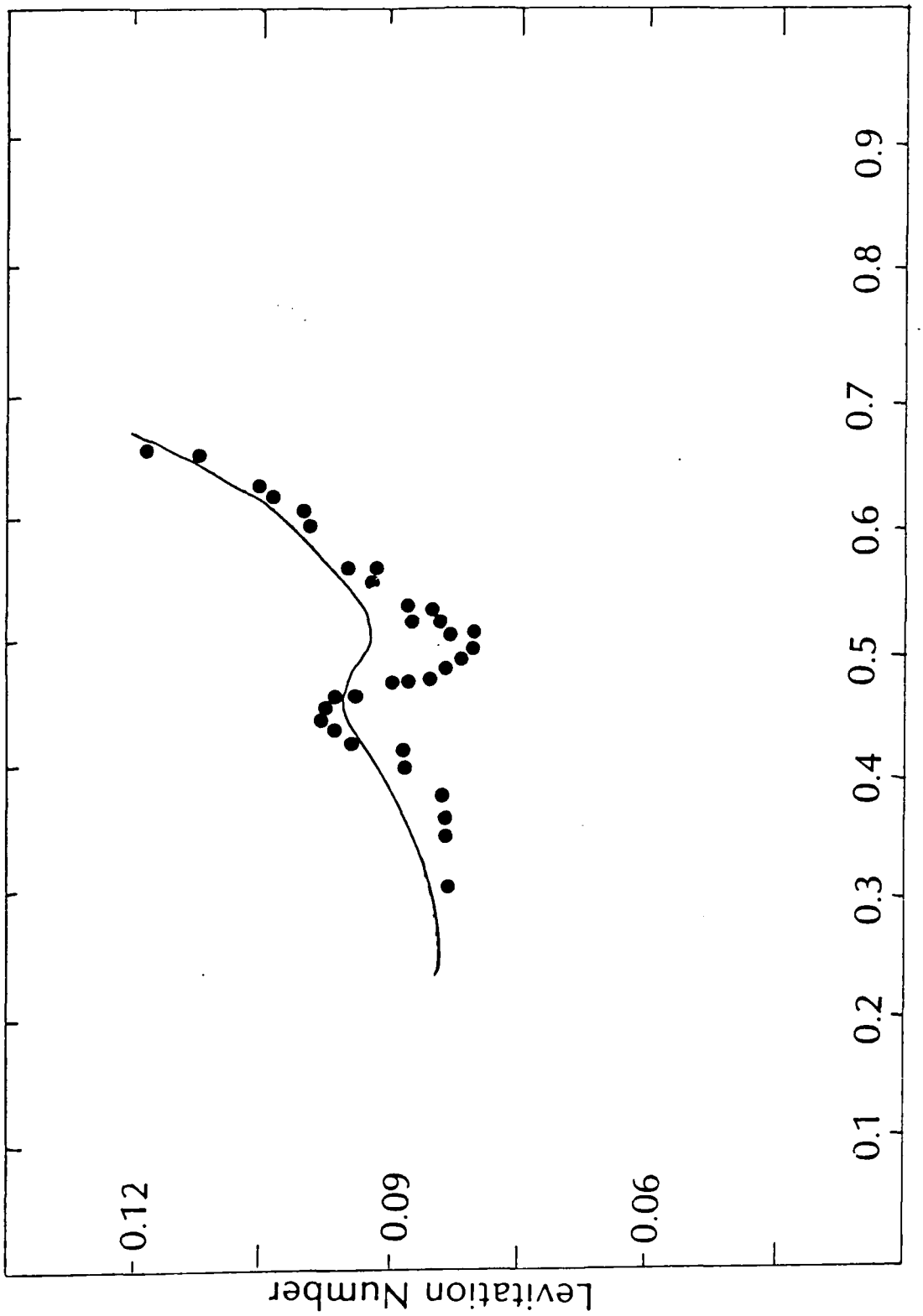

Fig. 9. Variation of levitation number with normalized bubble radius for glycerine/water mixture at 39°C.

Data was taken for the glycerine/water mixture for a variety of temperatures, some as high as 62° C. Because of the large difference in temperature between the ambient air and the liquid in the cell, data was very difficult to obtain at the higher temperatures. Convection currents and variable gas content levels, in addition to evaporation, caused many delays and complications. Shown in Figs. 10 and 11 are data obtained in the "high" temperature region.

The data shown in Fig. 10 represent a bubble in glycerine/water at 49.5° C. The acoustic pressure amplitude was 0.16 bars. The levitation number in the small bubble region is almost constant at 0.08, indicating as in the previous data, a linear dependence on acoustic pressure which agrees with the theory. The levitation number in the range of harmonic resonance changes from a maximum of about 0.09 to a minimum of about 0.08, which, when compared to Fig. 7 with the same acoustic pressure amplitude of 0.16 bars, shows a considerable reduction in range. In Fig. 7, with the same pressure amplitude but with a temperature of 35° C, the range of the levitation number over the harmonic resonance was from a maximum of about 0.10 to a minimum of about 0.08. This change is related to the higher temperature, which among other things, should affect the damping. Preliminary calculations indicate that the effect of the additional vapor in the bubble is to increase the damping. For bubbles of large size, the agreement with theory is not as good as in the data taken at lower temperatures. This effect may be due to the difficulty of measuring the correct radius of the larger bubbles. Large bubbles in the liquid at relatively high temperatures tended to grow very rapidly to resonance size

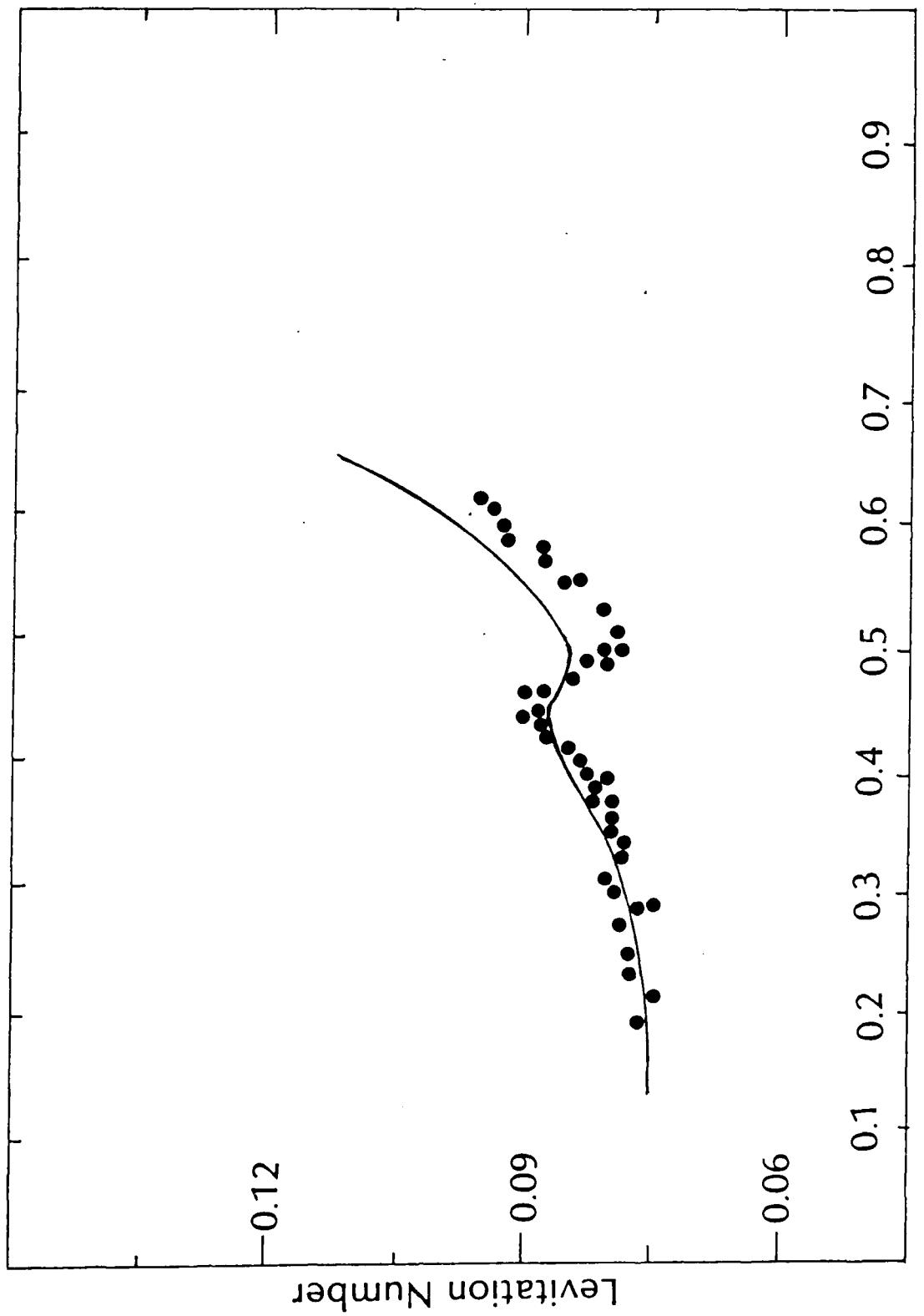

Fig. 10. Variation of levitation number with normalized bubble radius for glycerine/water mixture at 49.5°C.

and so data acquisition was more difficult than at lower temperatures.

In Fig. 11, data is shown for a temperature of 50° C. In this case bubbles of large radius were not obtained; however, the range of the levitation number in the region of 0.4 to 0.5 normalized radius was from a maximum of about 0.14 to a minimum of about 0.10. This wide range is due to the relative large acoustic pressure amplitude of 0.22 bars. The smaller bubbles in this particular figure show a wide distribution of levitation numbers. This effect was probably a result of the currents in the liquid at such high temperatures. It is apparent from the data presented in Figs. 7 through 11 that the levitation number is affected considerably by the temperature of the host liquid.

In addition to the glycerine/water mixture, isopropyl alcohol was also used as a host liquid. The frequency used was near 20.5 kHz. Temperature was varied from 9° C to 30° C, while acoustic pressure amplitudes ranged from 0.075 to 0.23 bars. Fig. 12 shows data taken a 9° C with an acoustic pressure amplitude of 0.08 bars. As with the glycerine/water, small bubbles in the range of 0.3 to 0.4 for normalized radius were used to calibrate the cell for each data set. These small bubbles have a nearly constant levitation number of 0.04 which agrees well with the theory, indicated by the solid curve. In the region of normalized radius from 0.4 to 0.55, the levitation number changes from a maximum of about 0.046 to a minimum of about 0.044. These data in isopropyl alcohol are similar to those in glycerine/water in that again the theory predicts a much smaller variation in the levitation number than is observed, even for this case in which the amplitude of the variation

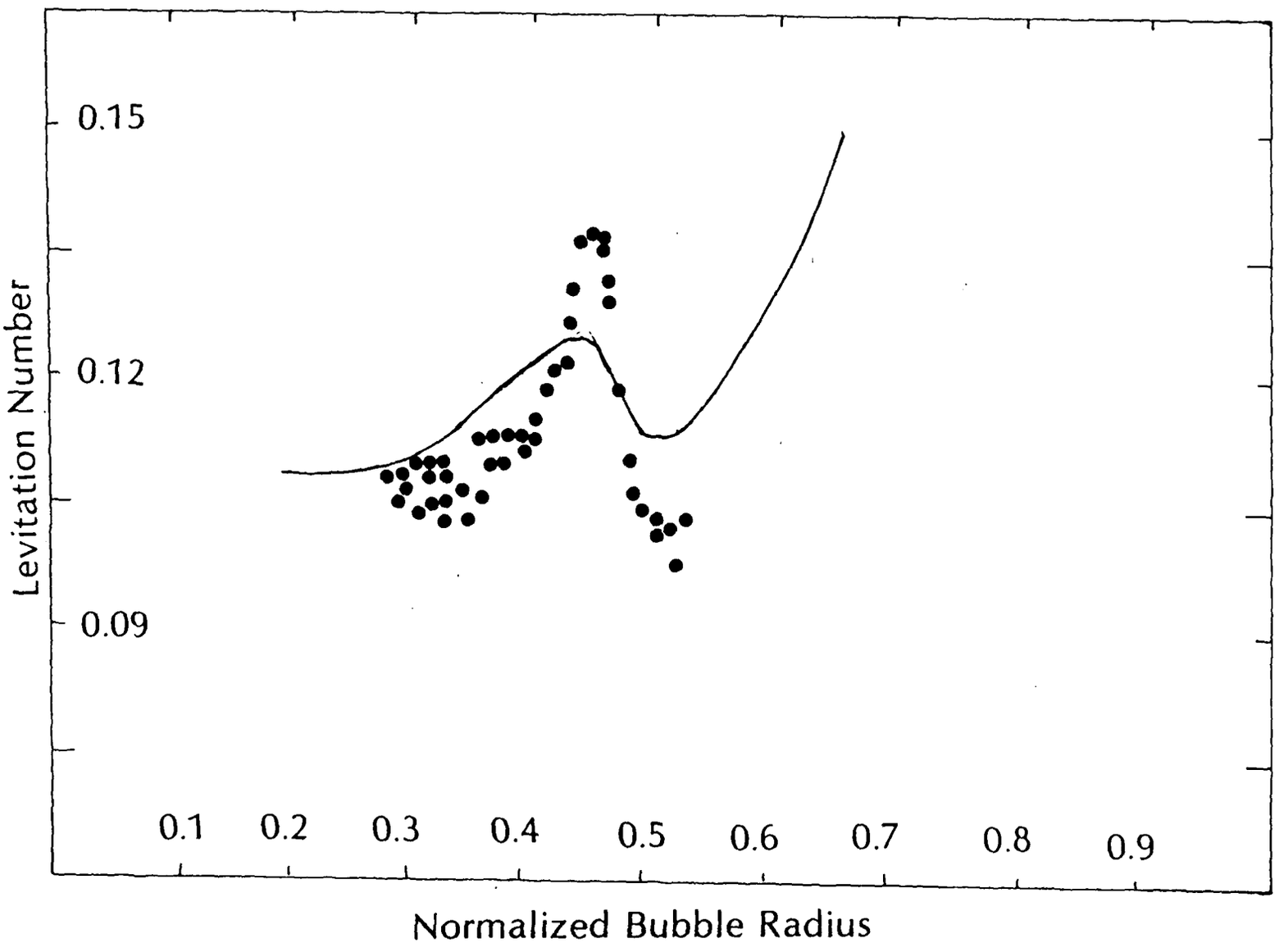

Fig. 11. Variation of levitation number with normalized bubble radius for glycerine/water mixture at 50° C.

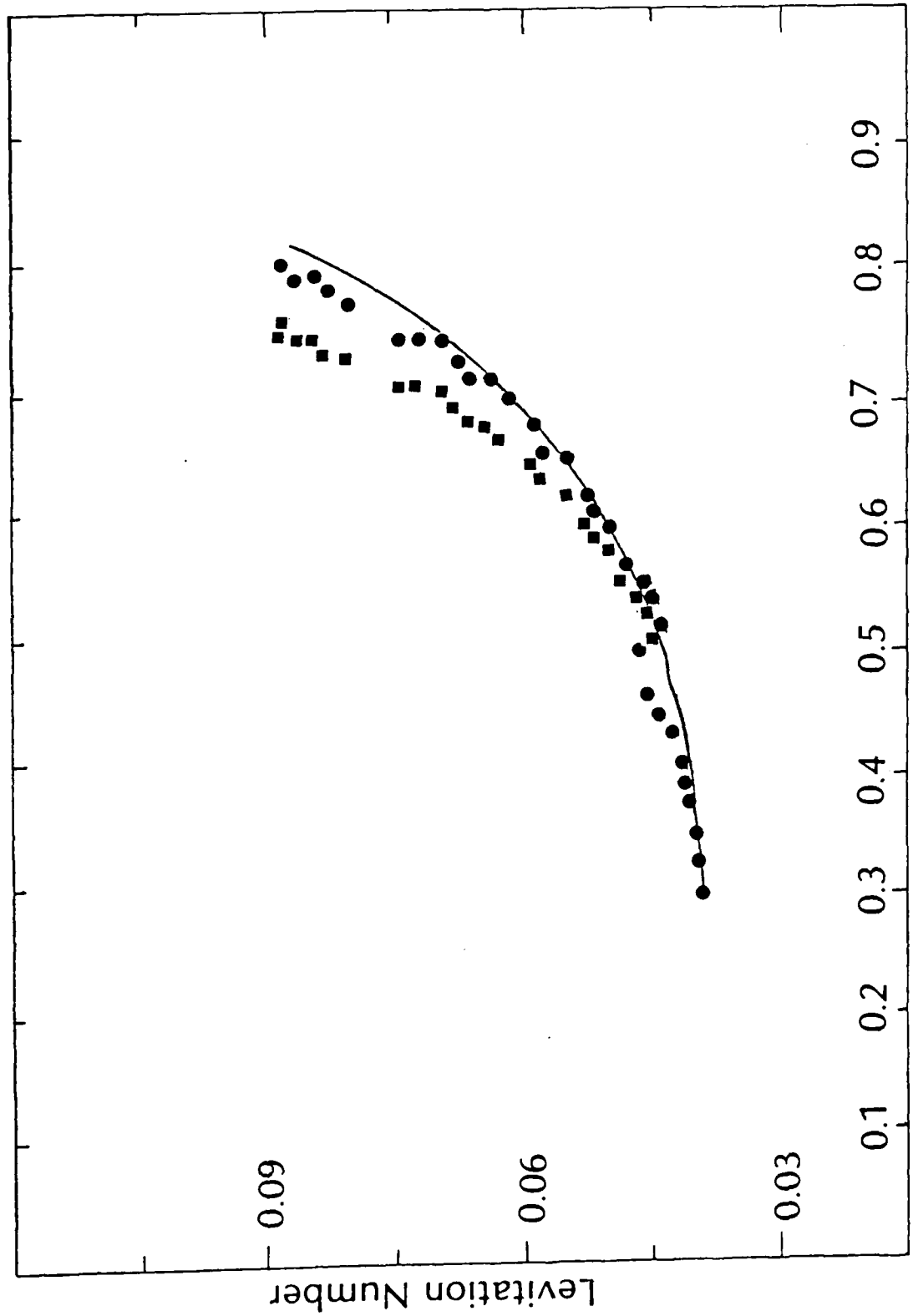

Fig. 12. Variation of levitation number with normalized bubble radius for isopropyl alcohol at 9°C.

is small. If the data are examined away from the harmonic resonance region, the match with theory is quite good. At this low temperature, it was possible to obtain a very wide range of bubble radii. The two different symbols on this figure refer to two different drag laws that were used. The solid circles refer to a solid sphere drag law whereas the squares refer to a fluid sphere law.

Fig. 13 shows data taken for a temperature of 15° C with an acoustic pressure amplitude of 0.12 bars. The linear portion of the graph for small bubble radii shows a near constant levitation number of about 0.056 which, when compared to the other figure shown, shows that increasing the acoustic pressure amplitude increases the levitation number. The experimental data again agree with theory for small bubbles and large ones, but is not in agreement in the region of the harmonic resonance.

In Fig. 14, the data was taken at 20° C. The acoustic pressure amplitude was 0.12 bars and the levitation number for the small bubbles with normalized radius less than 0.4 was a nearly constant 0.056 which agrees with the levitation number for the same region in Fig. 13 (same acoustic pressure amplitude). As the bubble grew to the region of the harmonic resonance the levitation number again changed much more than the theory predicted. After the bubble reached 55% of resonance radius, there was again agreement with theory. The fact that the magnitude of the oscillation in the levitation number near the harmonic resonance is considerably larger at 20° C than at 15° C, while the acoustic pressure amplitudes

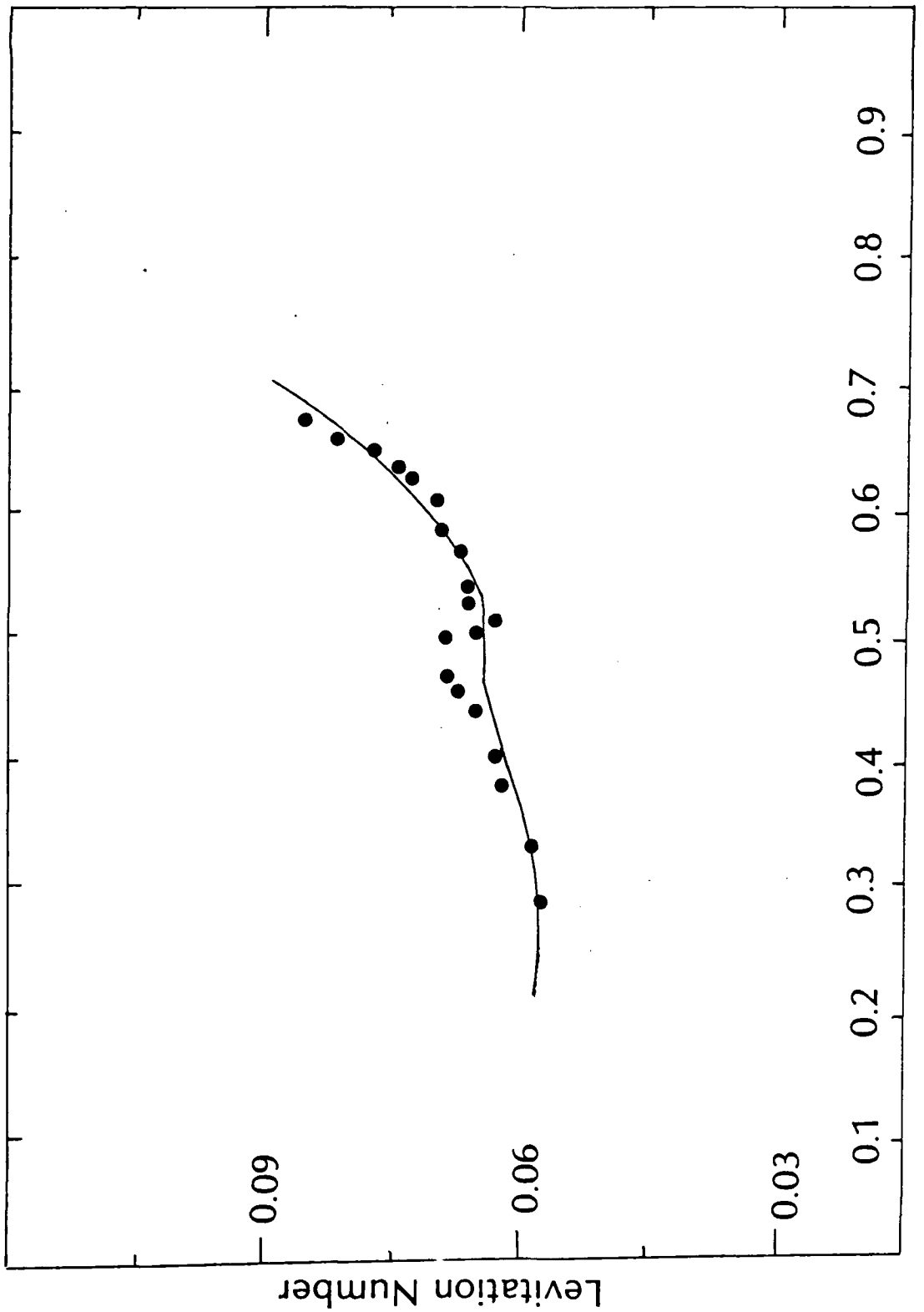

Fig. 13. Variation of levitation number with normalized bubble radius for isopropyl alcohol at 15°C.

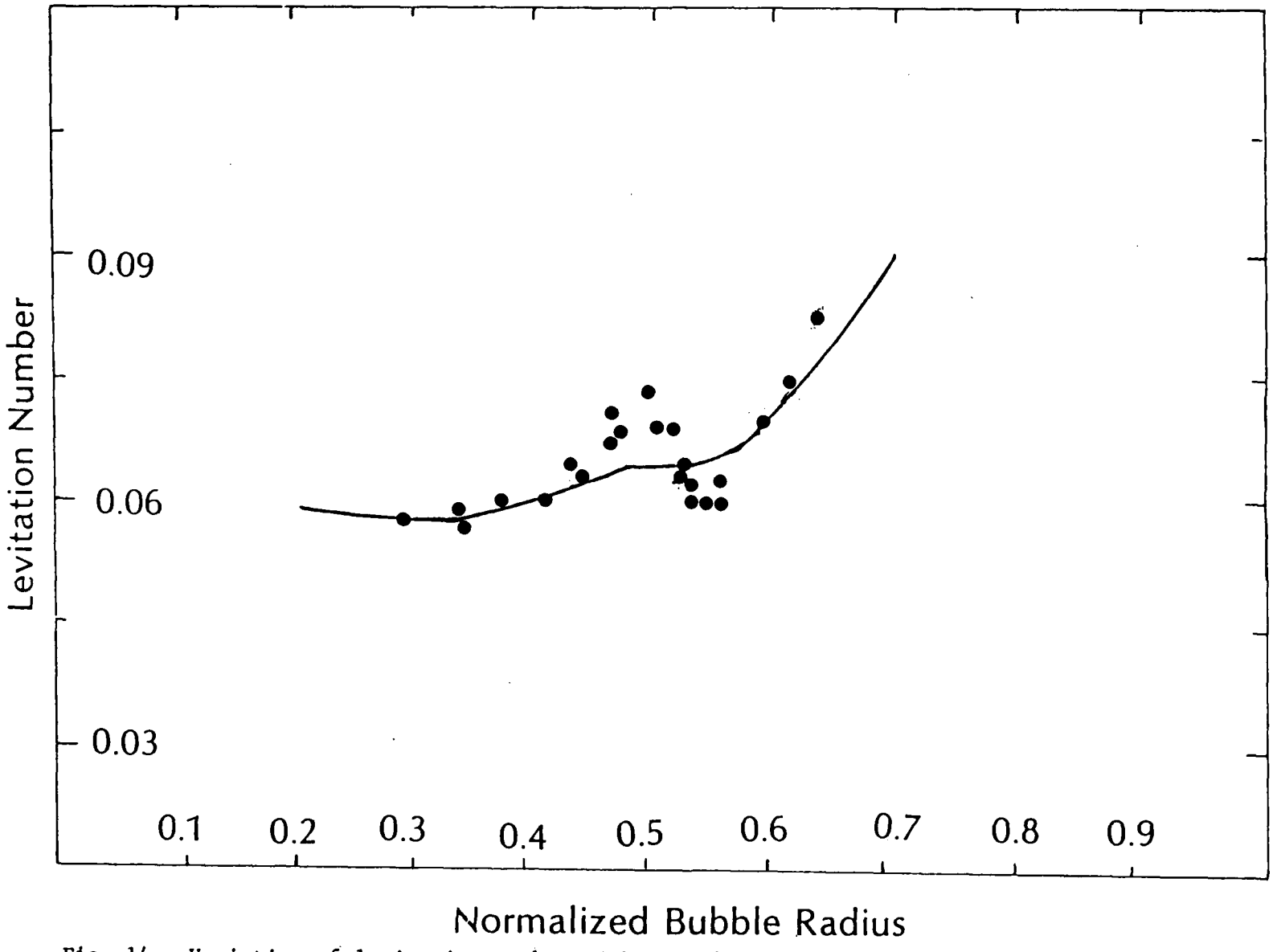

Fig. 14. Variation of levitation number with normalized bubble radius for isopropyl alcohol at 20°C.

remained the same, indicates that the presence of small amounts of additional vapor inside the bubble significantly affects its nonlinear response.

Fig. 15 shows data taken at 26° C with an acoustic pressure amplitude of 0.105 bars. The levitation number for small bubbles in the linear region is near 0.05. This value is less than those in Figs. 13 and 14 which is expected due to the reduced acoustic pressure amplitude.

It is difficult to compare the glycerine and water data with the isopropyl alcohol data since the acoustic pressure amplitudes were not the same. The acoustic pressure amplitude was determined in part by the liquid itself, and it was not possible to select a value before a run was made. Even though several data runs were made, a set of data investigating the variation in levitation number with temperature for fixed acoustic pressure amplitude was never obtained. Furthermore, because the liquid's physical properties have an effect on the magnitude of the levitation number, comparisons of data sets for the same values of the temperature and acoustic pressure cannot realistically be made.

All figures show strong agreement between experimental data and theory for the regions above 55% and below 40% of resonance radius, that is,in the linear regions. The principal area of concern is the region near the harmonic resonance. In Fig. 16, a typical set of experimental results, using the glycerine/water mixture, is shown. The linear theory prediction is shown by the dashed line and the nonlinear theory showing a combination of contributions from the individual resonance regions,

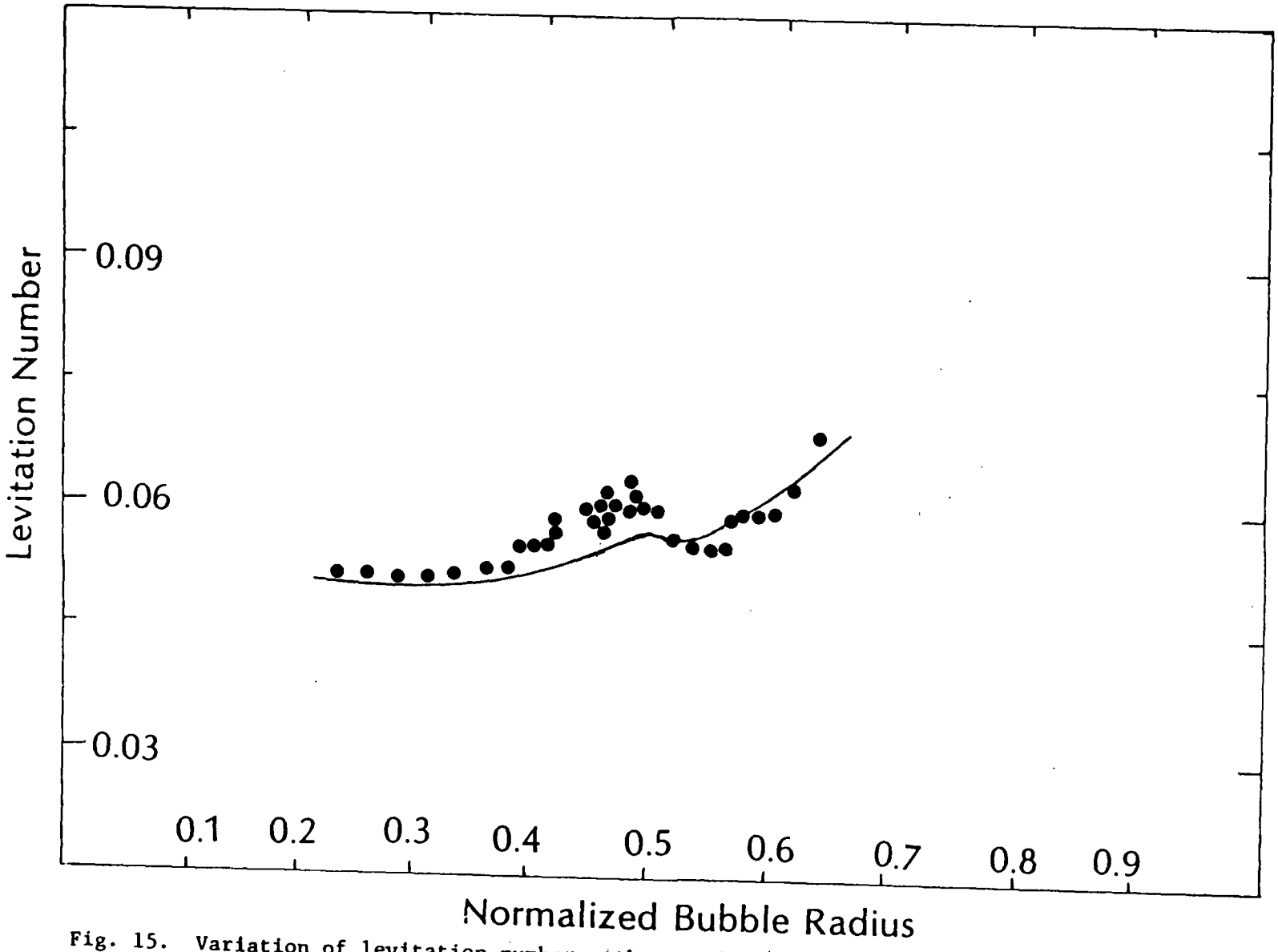

Fig. 15. Variation of levitation number with normalized bubble radius for isopropyl alcohol at 26°C.

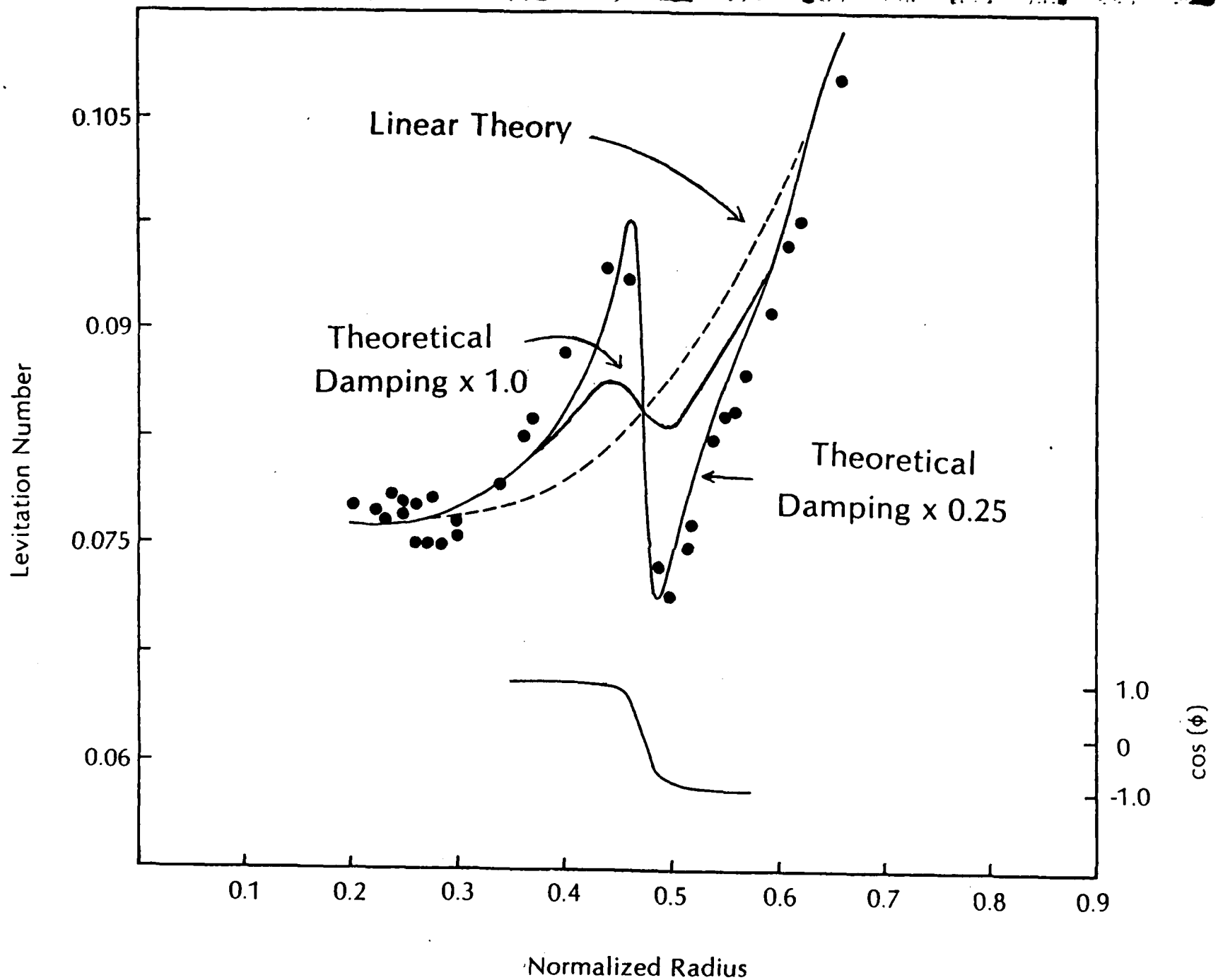

Fig. 16. Variation of levitation number with normalized bubble radius for different values of the damping constant.

is indicated by the solid line marked with Damping x 1.0. The other solid line marked Damping x 0.25 shows how the theoretical values changed when the damping was reduced by a factor of 4. This results in a very close fit with experimental data. The areas which agreed before continue to do so and the region of principal concern now matches nicely with theory. The fact that this simple adjustment in the damping creates such good agreement indicates a flaw in the theory. Although it would be easy to attribute this discrepancy to an incorrect evaluation of the damping, such an assumption is probably unwarranted. Independent measurements of bubble damping show no discrepancy with theory, and to expect one here is not reasonable. What is probably occurring is that the polytropic exponent, which is treated with a linear theory, must also be examined nonlinearly, in order to assign it an appropriate value in this highly nonlinear region. Also shown in the figure are the variations of the phase angle ϕ as a function of radius. The rapid change in the phase angle in the region of harmonic resonance is the main cause for the rapid change of levitation number near the normalized radius value of 0.5.

It is clear that work needs to be done in the theoretical area. The experimental measurements required to evaluate the levitation number are quite straightforward, and thus there is little cause to expect the values of the levitation number to be in error. An examination of the theory in a completely nonlinear way is, however, a very difficult task and cannot be done quickly. Yet, these data show that some interesting and important effects are being observed that offer

real challenges for future research work.

ANALYSIS OF ERRORS AND ACCURACY

Errors in this experiment could rise from several areas. In the direct measurements involved in each data set -- the temperature, frequency, bubble position, rise velocity and acoustic pressure -- are of major concern. In addition to these values, physical constants associated with the liquids and gases were utilized. In some cases, these values were obtained from references and in other instances, the values were measured experimentally. Examinations of each area for possible error follow.

The values used as constants were, in general, very accurate for the temperature used. The difficulty arose in the fact that temperature was measured to an accuracy of 0.2° C, giving an error of 0.7% over the range of temperatures used. If the viscosity for isopropyl alcohol at 30° C was obtained from a table, this value was valid for that temperature but the temperature of the liquid could have been different from measured values or could have changed over the period of data acquisition. To avoid error related to this circumstance, temperature measurements were made before and after data collection and data was taken over as short a time as possible, on the average of 30 minutes. In order to determine the effect on the levitation number or the normalized radius of an inprecision in one of the many constants and variables used in their calculation, a sensitivity analysis was performed. That is, the parameter under consideration was varied by an amount equal to its inprecision and

then the applicable computer program was utilized to test the effect of this variation on the levitation number or normalized radius. For example, viscosity was measured to an accuracy of ±0.1%. Substituting the two values of viscosity into the computer program resulted in a change in the normalized radius of 0.04% and had very little effect on the levitation number. Thus, the levitation number and the normalized radius were rather insensitive to errors in the measurement of the viscosity.

The values relating to the properties of the acoustic wave in the cell were determined by calibration of the cell with a probe hydrophone. The errors involved in these values were a result of various factors. The probe itself tended to change the sound field and the level of the liquid. Other considerations related to the voltage and position measurement will be mentioned later. These factors were counteracted, to a degree, by the use of a calibration routine using small bubbles in linear oscillations. This was done for each data set. The measured wavelength of the acoustic signal was a critical factor and was accurate to only 1.1%. This results in a variation of the levitation number by a value of 1%.

Another area of concern relating to the error in values used for constants is that when the mixture of glycerine and water was used, values of the viscosity were obtained from measurements already mentioned. These measurements, even though they fit well in between, viscosity values of known mixtures were probably less accurate than textbook values.

In the area of measured values, the frequency, which was continually tuned to the correct resonance value , was accurate to within 0.05%. This error resulted in no measurable effect on the calculated radius or the levitation number. The values of rise time were accurate to 0.01 seconds as a result of the methods used to obtained measurement. The bubble was positioned in the field of view and its position was recorded. Then the sound was discontinued and the bubble was allowed to rise a certain distance, as indicated by the fiducial lines in the microscope. It could be determined that the bubble was not changing size by the fact that rise-times could be repeated within 0.02 seconds several times. This inaccuracy of the time resulted in a maximum 0.3% error in the calculated normalized radius. An effort was made to keep rise times around 2 seconds since longer times could result in a change in bubble radius during its rise while shorter times increased the relative error.

The bubble position was determined by use of the cathetometer (accurate to 0.02%). This reading, when related to absolute displacements within the levitation cell, would give information relating the position of the bubble in the sound field to the distance the bubble traveled during the given rise time. The location of the bubble in the sound field was used to determine the bubble radius to an accuracy of 0.03% and this information was used to give a levitation number, accurate to 0.07%.

Bubble displacement as measured through the use of fiducial lines in the microscope was accurate to 0.1 line which gives an accuracy of 1.2% since the bubble was allowed to rise an average of 2 seconds. This

translates to bubble movement of between 1 mm and 16 mm. The accuracy results in a radius variation of 1.4%.

Voltage, which was a measure of the acoustic pressure amplitude in the cell, was held constant during data collection but was periodically checked. The voltage would only change when the bubble grew to resonance. An accuracy of 0.001 volts results in 0.2% error. The fluctuation of voltage was an indication of the presence of additional bubbles. These bubbles usually were levitated near another antinode or on the surface of the cell. If these bubbles were present, they would tend to disrupt the sound field if they grew to resonance size. Data was not taken when the additional bubbles were present.

The calculations of bubble radii and levitation number are very complex as shown by the computer program 1 in Appendix A. The resulting errors in experimental data could be as high as 20% in some instances, but the values shown are in such strong agreement with theory, in the applicable regions, that it is felt that a 5% error would be more appropriate.

CONCLUSIONS

A unique and sensitive technique has been developed for the study of nonlinear oscillations of an individual bubble in liquid. Measurement of various aspects of the individual bubble's behavior is possible with this levitation technique. The technique has been very successful in the limited study explained in this paper and much promise is shown for future study. These measurements may be made with little difficulty after some experience is gained using this technique.

The fit of experimental data with theory is consistent throughout the various data samples shown for the regions of normalized radius less than 0.4 and more than 0.55. Theory and experiment do not agree in the region of the n=2 harmonic unless the damping is reduced by a factor of 4. The reasons for this discrepancy are unclear and more study is needed in this area.

REFERENCES

1. A. I. Eller, J. Acoust. Soc. Amer. 43, 170-171 (L) (1968).

2. R. E. Apfel, J. Acoust. Soc. Amer. 59, 339 (1976).

3. L. A. Crum and A. I. Eller, "The Motion of Bubbles in a Stationary Sound Field," Tech. Memo. No. 61, Acoust. Res Lab, Harvard Univ. (1969).

4. L. A. Crum, J. Acoust. Soc. Amer. 68, 203-211 (1980).

5. R. E. Apfel, New Scientist 84, 857-859 (1979).

6. L. A. Crum, J. Acoust. Soc. Amer 57, 1363-1370 (1975).

7. E. W. Washburn (ed.), International Critical Tables of Numerical Data, Physics, Chemistry and Technology, New York (1928).

8. R. W. Gallant, Physical Properties of Hydrocarbons Volume 1, Houston, Texas (1968).

9. R. J. Pelt, "Viscosity Prediction for Binary Mixtures," Oxford, MS (1960).

10. A. J. Moses, The Practicing Scientist's Handbook: A Guide for Physical and Terrestrial Scientists and Engineers, New York (1978).

11. R. C. Weast (ed.), CRC Handbook of Chemistry and Physics, Boca Raton, Florida (1981).

12. A. C. Merrington, Viscometry, Longmans, Green & Co., New York (1949).

13. L. A. Crum and A. Prosperetti, J. Acoust. Soc. Amer. 73, 116-120 (1983).

14. A. I. Eller, J. Acoust. Soc. Amer. 47, 1469-1470 (1970).

15. C. Devin, J. Acoust. Soc. Amer. 31, 1654-1667 (1959).

16. A. Prosperetti, J. Acoust. Soc. Amer. 61, 17-21 (1977).

17. L. A. Crum, J. Acous. Soc. Amer. 73, 116-120 (1983).

18. A. Prosperetti, J. Acoust. Soc. Amer. 56, 878-885 (1974).

APPENDIX A

COMPUTER PROGRAM 1

```
      INTEGER N,CONST,J5,Q5
       REAL A8,B8,C8,E8,F8,G8,A9,B9,C9,D9,ETAEX,SLO
       REAL Q6,W4,W5,W6,V6,W7,V7,W8,V8,R9
       REAL EE,EP,YE,YP,PE(200),PP(200),WE(200),WP(200)
       REAL PE3(200),PP3(200),C6(200),CON,PAE(200),AP(200)
       REAL B1,B2,B3,S5(200),E5(200),R5(200),R7(200),R2(200)
       REAL A5,F5(200),H5(200),G5(200),K,R6,R8(200),W0,RAT,ETA1
       REAL F7(200)
       REAL SUR,DEL,PZ,ET,EA,DIF,ETA2
      REAL C0,M1,M2,L5,S1,T1,Q1,T5(200),C5(200),V(200),D5(200)
      REAL*8  M,D1,T,F,G,R1,W,G1,X
         REAL*8 U,P0,C1,DV,DR,DT,X1,DT1,DT2,E1
           REAL*8 DT3,E2,DE,DP,ETA,C2
      REAL*8 G2,A,B,C,D,E,H,I,J,L,Y1,Y2,Y
      REAL*8 Z1,Z,Z2,Q,KAP,DPV,DPR,DPT
      FNC(X)=(DEXP(X)+DEXP(-X))/2
      FNS(X)=(DEXP(X)-DEXP(-X))/2
      READ (9,10) CON,M1,M2,L5
       READ (9,13) S1,T1,Q5
       READ(9,10) B1,B3,B5,U
       READ(9,10) G,F,C1,C2
       READ (9,10) M,D1,R9,SUR
  250  FORMAT(' 123,LAM,#,C0 AND SLO')
  220  FORMAT(I)
  390  FORMAT(2F)
  400  FORMAT(' L5 AND C0 =  ')
   10  FORMAT(4F)
   13  FORMAT(2F,1I)
 17    FORMAT(3F)
   16  FORMAT(2F)
       TYPE 250
       ACCEPT 220,CONST
       ACCEPT 300,L5
       ACCEPT 220,Q5
       ACCEPT 300,C0
       ACCEPT 300,SLO
       IF (CONST.LE.2) GO TO 83
       TYPE 312
 312   FORMAT('              N       RADIUS       ETAEX
     1      ETA-ITE          KAPPA')
```

```
83      CONTINUE
        IF (CONST.GE.3) GO TO 22
        TYPE 310
 310    FORMAT('                    N  NOR-RAD   P-ELLER
     1ALPHA-PRI')
 22     READ (9,120) (T5(N),C6(N),V(N),D5(N),N=1,Q5)
120    FORMAT(4F)
300     FORMAT (1F)
        P0=1.0E6
        T=273+T1
       R1=8.3D7
 190    K=6.2832/L5
       W=2.*3.14159*F
       G1=M*D1*W/(G*G*R1*T)
        DO 180 N=1,Q5
        C5(N)=(C6(N)-C0)*M1

        S5(N)=D5(N)*M2
        E5(N)=S5(N)/T5(N)
        R5(N)=1.0E-3
 36     R7(N)=2.*R5(N)*E5(N)*C2/U
        R2(N)=1.+0.197*R7(N)**0.63+(2.6E-4)*R7(N)**1.38
        R5(N)=SQRT(4.5*U*E5(N)*R2(N)/(980*C2))
        A5=SQRT((R5(N)-R6)**2)
        IF (A5.LE.1.0E-5) GO TO 40
        R6=R5(N)
        GO TO 36
 40     CONTINUE
       R5(N)=1.000*R5(N)
        F5(N)=B1*SIN(K*C5(N))+B3*SIN(3*K*C5(N))
     1   +B5*SIN(5.*K*C5(N))
        H5(N)=5*B5*COS(5*K*C5(N))
        G5(N)=K*(B1*COS(K*C5(N))+3*B3*COS(3*K*C5(N))+H5(N))
       G2=W*R5(N)*R5(N)/D1/G
       A=((G-1)/G)*(G1/2.)
       B=DSQRT(G1*G2)
       C=DSQRT(G*G2/2.)
       D=2.*C*(1-A)
        E=2.*C*(1+A)
       H=FNC(D)-DCOS(E)
       I=FNC(2.*A*B)-DCOS(2.*B)
       J=B*(A*G1/G-1)
       L=B*(A+G1/G)
        Y1=2.*A*I*(D*FNS(D)+E*DSIN(E)-2.*H)
        Y2=2.*H*(J*FNS(2.*A*B)+L*DSIN(2.*B)-I*G1/G)
        Y=Y1-Y2
        Z1=2.*A*I*(E*FNS(D)-D*DSIN(E))
```

```
Z2=2.*H*(L*FNS(2.*A*B)-J*DSIN(2.*B)-I)
Z=Z1-Z2
Q1=2.*H*I*(G1*Y/G-2.*A*Y+Z)
Q=Q1/(Y*Y+Z*Z)
KAP=G*G1*G2*Q/3.E0
   X1=R5(N)*DSQRT(2.*W/D1)
   DT1=X1*(FNS(X1)+DSIN(X1))-2.*(FNC(X1)-DCOS(X1))
    DT3=FNS(X1)-DSIN(X1)
   DT2=X1*X1*(FNC(X1)-DCOS(X1))+3.*(G-1.)*X1*DT3
    DT=3.*(G-1.)*DT1/DT2
  E2=(FNC(X1)-DCOS(X1))*X1
    E1=3.*(G-1)*(FNS(X1)-DSIN(X1))/E2
    ETA=G/((1+DT*DT)*(1.+E1))
     DR=C2*R5(N)**3.*W**3./(3.*ETA*P0*C1)
    DV=4.*W*U/(3.*ETA*P0)
DE=DV+DT+DR
 DP=(Y-Z*G1/G-2.*A*Z)/(G1*Y/G-2.*A*Y+Z)
DPV=DV
 DPR=DR/(1.+(W*R5(N)/C1)**2.)
  DPT=DPV+DPR+DP
EE=SQRT(C2/3./ETA/P0)*R5(N)*W
EP=SQRT(C2/3./KAP/P0)*R5(N)*W
YE=((1-EE**2.)**2.+DE**2)/(1-EE**2.)
YP=((1-EP**2.)**2.+DPT**2.)/(1-EP**2.)
PE(N)=SQRT(2*ETA*C2*980*P0/F5(N)/G5(N)*YE)
PP(N)=SQRT(2*KAP*C2*980*P0/F5(N)/G5(N)*YP)
PE(N)=1.0E-6*PE(N)
PP(N)=1.0E-6*PP(N)
WE(N)=V(N)/PE(N)/SLO
WP(N)=V(N)/PP(N)/SLO
 PAE(N)=(V(N)/SLO)*P0
 AP(N)=2*C2*980/(3*PAE(N)*G5(N))
PE3(N)=PE(N)*F5(N)
PP3(N)=PP(N)*F5(N)
F7(N)=AP(N)/PE3(N)
A8=C2*W*W*R5(N)*R5(N)/(3*P0)
B8=DT
C8=C2*(R5(N)**3)*(W**3)/(3*P0*C1)
D8=4*W*U/(3*P0)
E8=2*C2*980.*P0/(F5(N)*G5(N))
G8=C8+D8
P8=(V(N)/SLO)*P0
F8=(P8*P8)/E8
A9=1.+B8*B8
B9=2*G8*B8-2*A8-F8
C9=G8*G8+A8*A8+F8*A8
D9=SQRT(B9*B9/(4*A9*A9)-C9/A9)
```

```
          R8(N)=R5(N)/R9
          PZ=P0+2*SUR/R5(N)
            ET=2*SUR/(3*PZ*R5(N))
          ETA2=KAP
  611     W0=SQRT((3*ETA2*PZ-2*SUR/R5(N))/(C2*R5(N)**2))
          DEL=ATAN(W*W0*DPT/(W0*W0-W*W))
          RAT=(1.-W*W/(W0*W0))**2+(W*DPT/W0)**2
          EA=2*C2*980*PZ*SQRT(RAT)
              ETA1=P8**2*F5(N)*G5(N)*COS(DEL)/EA+ET
          DIF=SQRT((ETA2-ETA1)**2)
          IF (DIF.LE.1.0E-3) GO TO 612
          ETA2=ETA1
  612     ETAEX=D9-B9/(2*A9)
          IF (CONST-2) 280,180,290
   290    TYPE 130,N,R8(N),ETAEX,ETA1,KAP
          IF (CONST.EQ.3) GO TO 180
   280    TYPE 130,N,R8(N),PE3(N) ,AP(N),V(N),WE(N)
    130   FORMAT(1I,5F10.6)
   180    Q6=Q5
          W4=0
          W5=0
          V4=0
          V5=0
          V7=0
          W7=0
          IF (CONST.EQ.3) GO TO 350
          DO 140 N=1,Q6
          W4=W4+WE(N)
    140   V4=V4+WP(N)
          W6=W4/Q6
          V6=V4/Q6
          DO 150 N=1,Q6
          W7=W7+(WE(N)-W6)**2
    150   V7=V7+(WP(N)-V6)**2
          W8=SQRT(W7/(Q6-1))
          V8=SQRT(V7/(Q6-1))
          TYPE 170,C0,W6,W8
          IF (CONST.EQ.2) GO TO 420
          TYPE 400
          TYPE 390,L5,C0
    170   FORMAT(3F14.6)
    200   FORMAT(1I,1F12.6)
   420    C0=C0-1
          IF (CONST.EQ.1) GO TO 350
          IF (L5.LE.29.) GO TO 190
          IF(C0.LE.0.) GO TO 190
   350    CONTINUE
          STOP
         END
```

APPENDIX B

COMPUTER PROGRAM 2

```
C*****************************************************************
C
C     THIS PROGRAM COMPARES OUR EXPERIMENTAL DATA WITH THE THEO
C     RY
C     OF ANDREA PROSPERETTI.  IT CALCULATES A BUBBLE'S MAXIMUM
C     CHANGE IN RADIUS AS A FUNCTION OF FREQUENCY FOR RESONANCE
C     AND THE FIRST AND SECOND HARMONICS.
C*****************************************************************

      COMMON AAZ
      COMMON/WR/AMPL(3),COSPH
      REAL XMAX1(3),XMAX2(3)
      DATA W0,W1,W2,XMAX0,XMAX1,XMAX2/10*0./
      RRES=0.0174
      R=0.20*RRES
C**** INITIALIZING CONSTANTS ***********************************

      GAMMAP=1.40
      BIGD1=.205
      SIGMA=22.0
      PINF=1000000.0
      ROE=.7800
      DELTR0=.01
      DELTR1=.005
      TYPE 137
137   FORMAT(' INPUT PA')
      ACCEPT 135,PA
135   FORMAT (1F)
      TYPE 136
136   FORMAT('   R/R0          LEV NUM          ALPHA PRIME')
      DFUDGE=0.000
                BIGO=20200*2*3.141596
      SPEED=161000.0
      AMU=0.022
      DO 100 I=1,300
      PROSP=R/RRES
      PROSP=R/RRES
      IF(PROSP.GT.0.76)GOTO 50
      ECKS=R*SQRT(2.*BIGO/BIGD1)
      QQZ1=(SINH(ECKS)-SIN(ECKS))/(COSH(ECKS)-COS(ECKS))
```

```
      QQZ2=(SINH(ECKS)+SIN(ECKS))/(COSH(ECKS)-COS(ECKS))
      DTHERM=3*(GAMMAP-1)*(ECKS*QQZ2-2)/ECKS
      DTHERM=DTHERM/(ECKS+3*(GAMMAP-1)*QQZ1)
      GAMMA=GAMMAP/(1+DTHERM**2)
      GAMMA=GAMMA/(1+3*(GAMMAP-1)*QQZ1/ECKS)
      GAMMA=1.0*GAMMA
      P0=PINF+2.*SIGMA/R
      DBLU=2.*SIGMA/(R*P0)
        ALPHA1=4.5*GAMMA*(GAMMA+1.)-2.*DBLU
        ALPHA2=.5*GAMMA*(9.*GAMMA**2.+18.*GAMMA+11.)-3.*DBLU
      BIG00=SQRT((3.*GAMMA*P0-2.*SIGMA/R)/(ROE*R*R))
      OMEGA0=R*BIG00*SQRT(ROE/P0)
      OMEGA=R*BIG0*SQRT(ROE/P0)
      DVIS=4.*BIG0*AMU/(3.*GAMMA*PINF)
      DRAD=ROE*(R*BIG0)**3/(3.*GAMMA*PINF*SPEED)
      DTOTAL=DTHERM+DVIS+DRAD+DFUDGE
      DCHECK=DTOTAL-DFUDGE
      B=.5*R*BIG0*DTOTAL*SQRT(ROE/P0)
      B=B*BIG00*BIG00/(BIG0*BIG0)
      ETA=PA/PINF
        XI=(1.-DBLU)*ETA
      AAZ=((OMEGA**2.-OMEGA0**2.)**2.+(2.*B*OMEGA)**2.)**-.5
      WRITE (23,20) DTHERM,DVIS,DRAD,DFUDGE,DTOTAL,DCHECK,B
20    FORMAT (' ',3X,7(E8.3,3X))
**** CALLING SUBROUTINES HRMNC1, HRMNC2, AND RESNCE **********

      WRITE (22,110) R,PROSP,B,DBLU,ETA,XI,OMEGA0
110   FORMAT (' ',E8.3,6(2X,E8.3))
      IF (PROSP.GE..20.AND.PROSP.LE..320) GO TO 200
160   IF (PROSP.GE..320.AND.PROSP.LE..600) GO TO 300
170   IF (PROSP.GE..600.AND.PROSP.LE.1.001) GO TO 400
      GOTO 140
200   CALL HRMNC2(ALPHA1,ALPHA2,B,OMEGA0,XI,W2,XMAX2,IERR2,OME
      GA)
      DELTAR=DELTR0
      XMAX2(3)=1.5*XMAX2(3)
      AMAX2=XMAX2(3)/1.5
       TYPE 410,PROSP,XMAX2(3),AMAX2
210   FORMAT(' ',3X,E10.5,4X,E10.5,4X,3(E10.5,3X))
      GOTO 160
300   CALL HRMNC1(PHASE,PHI,ALPHA1,ALPHA2,B,OMEGA0,XI,W1,
     /XMAX1,IERR1,OMEGA)
      DELTAR=DELTR1
      XMAX1(3)=1.5*XMAX1(3)
      AMAX1=XMAX1(3)/1.5
        TYPE 410,PROSP,XMAX1(3),AMAX1
      GOTO 170
```

```
 400     CALL RESNCE(ALPHA1,ALPHA2,B,OMEGA0,XI,W0,XMAX0,OMEGA)
         DELTAR=DELTR0
         XMAX0=1.5*XMAX0
         AMAX0=XMAX0/1.5
          TYPE 410,PROSP,XMAX0,AMAX0
 410     FORMAT(' ',1X,5(E11.5,3X))



         IF (IERR2.NE.0) WRITE (21,120) IERR2
         IF (IERR1.NE.0) WRITE (21,130) IERR1
 120     FORMAT (' ',' **ERROR NOTE IN HRMNC2**  ',I3)
 130     FORMAT (' ',' **ERROR NOTE IN HRMNC1**  ',I3)
140      R=DELTAR*RRES+R
 100   CONTINUE
  50   STOP
       END
 ************************************************************************

      THIS IS A SUBROUTINE TO BE USED WITH THE PROGRAM COMPARING

      OUR RESULTS WITH THOSE OF PROSPERETTI.  IT CALCULATES THE

      RESONANCE CURVE FOR THE SECOND HARMONIC REGION.

 ************************************************************************

      SUBROUTINE HRMNC2(ALPHA1,ALPHA2,B,OMEGA0,XI,Y,XMAX,IERROR,
      OMEGA)
      REAL XMAX(3),XOFTAU(2400),COEFFC(4),ROOTSR(3),
     /  ROOTSI(3)
      COMPLEX ROOTS(3)
        COMMON AAZ
      NDEG=3
      IERROR=0


        Y=OMEGA/OMEGA0

        D=1./(OMEGA0**2.-OMEGA**2.)
        C0=(D*(ALPHA1-4.5*OMEGA**2.)-.5)/(OMEGA0**2.-4.*OMEGA**2
        .)
        C1=(.5*D*(D*(ALPHA1-1.5*OMEGA**2.)-1.))/OMEGA0**2.
        C2=.5*(ALPHA1+13.5*OMEGA**2.)/(OMEGA0**2.-36.*OMEGA**2.)
        C3=(.5*D*(D*(ALPHA1+1.5*OMEGA**2.)-1.))/(OMEGA0**2.-
     /    4.*OMEGA**2.)
        C4=(D*(ALPHA1+4.5*OMEGA**2.)-.5)/(OMEGA0**2.-16.*OMEGA**
        2.)
```

```
      C5=(.5*(ALPHA1-13.5*OMEGA**2.))/OMEGA0**2.
      G0=ALPHA1*(2.*C5+C2)+13.5*OMEGA**2.*(.25-2.*C2)-.75*ALPH
      A2
      G1=-2.*ALPHA1*C1+C4*(.5-D*(ALPHA1-6.*OMEGA**2.))+
     /   1.5*(ALPHA2-.5*OMEGA**2.)*D**2.-D
      G2=C0*(D*(ALPHA1+3.*OMEGA**2.)-.5)
      G5=C3*(D*(ALPHA1+3.*OMEGA**2.)-.5)+.25*(1.-D*(ALPHA2+
     /   1.5*OMEGA**2.))*D**2.
      QUE3=9.*OMEGA**2.-OMEGA0**2.-XI**2.*(G1-G2)
***** INITIALIZING THE COEFFICIENTS FOR THE CUBIC "C**2." *****

      COEFFC(1)=G0**2.
      COEFFC(2)=2.*QUE3*G0
      COEFFC(3)=QUE3**2.+(6.*OMEGA*B)**2.
      COEFFC(4)=-1.*G5**2.*XI**6.
***** FINDING THE ROOTS OF "C**2." ******************************

      CALL ZPOLR (COEFFC,NDEG,ROOTS,IER)
***** ERROR CHECK ************************************************

      IF (IER.NE.0) IERROR=IER
***** LOOP TO FIND THE REAL ROOTS OF C**2 AND COMPUTE THE MAX.

***** VALUE OF XOFTAU FOR EACH OMEGA.

      DO 99 J=1,3
        ROOTSI(J)=AIMAG(ROOTS(J))
        ROOTSR(J)=REAL(ROOTS(J))
         IF (ROOTSI(J).EQ.0.) GO TO 98
           GO TO 99
 98     KSTOP=J*800
        KSTART=KSTOP
        X1=-6.*OMEGA*B*SQRT(ROOTSR(J))/(G5*XI**3.)
        X2=-SQRT(ROOTSR(J))*(QUE3+G0*ROOTSR(J))/(G5*XI**3.)
          PHI=ATAN2(X1,X2)
        TAU=0.
        R=.04/OMEGA
        DELTA=ATAN((2.*OMEGA*B)/(OMEGA**2.-OMEGA0**2.))
***** LOOP THAT CALCULATES XOFTAU. ******************************

        DO 88 K=KSTART,KSTOP
          THETA=3.*OMEGA*TAU+PHI
          XOFTAU(K)=SQRT(ROOTSR(J))*COS(THETA)+XI*((OMEGA**2.-
          OMEGA0
     /      **2.)**2.+(2.*B*OMEGA)**2.)**-.5*COS(OMEGA*TAU+DELT
          A)+(C1+
```

```
     /        C3*COS(2.*OMEGA*TAU))*XI**2.+(C5+C2*COS(2.*THETA))*
              ROOTSR
     /        (J)+(C4*COS(OMEGA*TAU+THETA)+C0*COS(OMEGA*TAU-THETA
              ))*XI*
     /        SQRT(ROOTSR(J))
             TAU=TAU+R
  88       CONTINUE
 ****  LOOP THAT FINDS THE MAX. VALUE OF XOFTAU.  ****************

          XMAX(J)=XOFTAU(KSTART)
          DO 77 L=KSTART,KSTOP
            IF (XMAX(J).LT.XOFTAU(L)) XMAX(J)=XOFTAU(L)
  77       CONTINUE
         XMAX(J)=XMAX(J)*COS(DELTA)
         BJERK=AAZ*XI*COS(DELTA)
         XMAX(J)=BJERK
 99        CONTINUE


       RETURN
       END
 ************************************************************************

       THIS IS A SUBROUTINE TO BE USED WITH THE PROGRAM COMPARING
       OUR DATA WITH THE RESULTS OF PROSPERETTI.  IT CALCULATES T
       HE
       RESONANCE CURVE FOR THE FIRST HARMONIC REGION.
 ************************************************************************

       SUBROUTINE HRMNC1 (PHASE,PHI,ALPHA1,ALPHA2,B,OMEGA0,XI,Y,X
       MAX,
      /IERROR,OMEGA)
       REAL XMAX(3),XOFTAU(2400),COEFFC(4),ROOTSR(3),
      /  ROOTSI(3)
       COMPLEX ROOTS(3)
         COMMON/WR/CC(3),X2
       COMMON AAZ
       NDEG=3

       IERROR=0

         Y=OMEGA/OMEGA0

         BIGD=1./(OMEGA0**2.-OMEGA**2.)
         C0=(BIGD*(ALPHA1-3.*OMEGA**2.)-.5)/(OMEGA0**2.-OMEGA**2.
         )
         C1=(.5*BIGD*(BIGD*(ALPHA1-1.5*OMEGA**2.)-1.))/OMEGA0**2.
         C2=(.5*(ALPHA1+6.*OMEGA**2.))/(OMEGA0**2.-16.*OMEGA**2.)
```

```
      C4=(BIGD*(ALPHA1+3.*OMEGA**2.)-.5)/(OMEGA0**2.-9.*OMEGA*
     *2.)
      C5=(.5*(ALPHA1-6.*OMEGA**2.))/OMEGA0**2.
      C6=2.*OMEGA*BIGD**2.
      BETA2=.5*BIGD*(BIGD*(ALPHA1+1.5*(OMEGA**2.))-1.)
      GZERO=ALPHA1*(2.*C5+C2)+6.*OMEGA**2.*(.25-2.*C2)-.75*ALP
     *HA2
      GONE=-2.*ALPHA1*C1+C4*(.5-BIGD*(ALPHA1-4.5*OMEGA**2.))+
     /   1.5*(ALPHA2-.5*OMEGA**2.)*BIGD**2.-BIGD
      GTWO=C0*(BIGD*(ALPHA1+1.5*OMEGA**2.)-.5)
      GTHREE=C6*(BIGD*(ALPHA1+1.5*OMEGA**2.)-.5)-2.*(BIGD**2.)
     *OMEGA
      QUETWO=4.*OMEGA**2.-OMEGA0**2.-(XI**2.)*(GONE-GTWO)
****  COMPUTING THE COEFFICIENTS OF THE CUBIC FUNCTION "C**2."

      COEFFC(1)=GZERO**2.
      COEFFC(2)=2.*GZERO*QUETWO
      COEFFC(3)=QUETWO**2.+(4.*B*OMEGA)**2.
      COEFFC(4)=-1.*(XI**4.)*BETA2**2.
****  CALLING THE SUBROUTINE "ZPOLR" TO SOLVE THE CUBIC. ******

        CALL ZPOLR (COEFFC,NDEG,ROOTS,IER)
****  ERROR CHECK ***************************************************

         IF (IER.NE.0) IERROR=IER
*****  LOOP TO FIND THE REAL ROOTS OF C**2 AND COMPUTE THE MAX.

*****  VALUE OF XOFTAU FOR EACH OMEGA.

      DO 990 KK=1,3
              XMAX(KK)=0.
               CC(KK)=0.
 990  CONTINUE
     DO 99 J=1,3
      ROOTSI(J)=AIMAG(ROOTS(J))
      ROOTSR(J)=REAL(ROOTS(J))
       IF (ROOTSI(J).EQ.0.) GO TO 98
        GO TO 99
98    KSTOP=J*800
      KSTART=KSTOP
      X1=B*SQRT(ROOTSR(J))*(GTHREE*(QUETWO+GZERO*ROOTSR(J))
     /   -4.*OMEGA*BETA2)/(XI*BETA2)**2.
      X2=-SQRT(ROOTSR(J))*BETA2*(QUETWO+GZERO*ROOTSR(J))/(XI*BE
     *TA2)**2.
       PHI=ATAN2(X1,X2)
     PHASE=COS(PHI)
      TAU=0.
```

```
      R=.04/OMEGA
      DELTA=ATAN(2.*OMEGA*B/(OMEGA**2.-OMEGA0**2.))
*****  LOOP TO CALCULATE XOFTAU  ***********************************

      DO 88 K=KSTART,KSTOP
        THETA=2.*OMEGA*TAU+PHI
       XOFTAU(K)=SQRT(ROOTSR(J))*COS(THETA)+XI*((OMEGA**2.-OMEG
       A0**2.)
     /    **2.+(2.*B*OMEGA)**2.)**-.5*COS(OMEGA*TAU+DELTA)+
     /    C1*XI**2.+(C5+C2*COS(2.*THETA))*ROOTSR(J)+(C4*COS(OMEG
          A*
     /    TAU+THETA)+C0*COS(OMEGA*TAU-THETA))*XI*SQRT(ROOTSR(J))
        TAU=TAU+R
88    CONTINUE
*****  LOOP TO FIND THE MAX. OF XOFTAU  ****************************

      XMAX(J)=XOFTAU(KSTART)
      DO 77 L=KSTART,KSTOP
        IF (XMAX(J).LT.XOFTAU(L)) XMAX(J)=XOFTAU(L)
77    CONTINUE
     XMAX(J)=XMAX(J)*COS(DELTA)
       CC(J)=SQRT(ROOTSR(J))
          CCC=CC(J)
       BJERK=AAZ*COS(DELTA)+CCC*C0*X2
       BJERK=BJERK+AAZ*(X2*COS(DELTA)+X1*SIN(DELTA))*CCC
       BJERK=XI*BJERK
       XMAX(J)=BJERK
99    CONTINUE
      RETURN
      END
*****************************************************************

      THIS IS A SUBROUTINE TO BE USED WITH THE PROGRAM THAT
      COMPARES OUR RESULTS WITH THOSE OF PROSPERETTI.  IT
      FINDS THE MAXIMUM OSCILLATION NEAR RESONANCE.
*****************************************************************

      SUBROUTINE RESNCE (ALPHA1,ALPHA2,B,OMEGA0,XI,W,XMAX,OMEGA)
        COMMON AAZ
        COMMON/WR/AMP,COSPH
      REAL XOFTAU(800)
      FAMP(X)=(OMEGA*B+.125*SIN(2.*X)*(XI/OMEGA0)**2.)/(XI*D3*SI
      N(X))+
     /  SQRT(((OMEGA*B+.125*SIN(2.*X)*(XI/OMEGA0)**2.)/(XI*D3*SI
      N(X)))
     /  **2.+1./D3)
      FPHI(Y,X)=Y*BOX-D1*Y**3.+XI*(1.-D2*Y*Y)*COS(X)+.25*Y*COS(2
      .*X)*
```

```
     /   (XI/OMEGA0)**2.
         W=OMEGA/OMEGA0
     **** PRELIMINARY EQUATIONS ************************************

         DEN=OMEGA0**2.-4.*OMEGA**2.
         D1=.75*ALPHA2-ALPHA1*(OMEGA0**-2.*(ALPHA1-1.5*OMEGA**2.)+
         .5*
     /   (ALPHA1+1.5*OMEGA**2.)/DEN)-1.5*OMEGA**2.*(.25-(ALPHA1+1
         .5*
     /   OMEGA**2.)/DEN)
         D2=.75*(ALPHA1-1.5*OMEGA**2.)/DEN+1.5*OMEGA0**-2.*(ALPHA1
         -.5*
     /   OMEGA**2.)-.75
         D3=.25*(ALPHA1-7.5*OMEGA**2.)/DEN+.5/OMEGA0**2.*(ALPHA1-1
         .5*
     /   OMEGA**2.)-.25
         BOX=OMEGA**2.-OMEGA0**2.-.5*(XI/OMEGA0)**2.*(2.*OMEGA**2.
          -
     /   OMEGA0**2.)/DEN
     ***** PROGRAMMING FOR FINDING THE PHASE ANGLE AND AMPLITUDE ***

     ***** OF OSCILLATION                                          ***

         J=0
         AAA=6.282
         ACHNGE=.06282
         F1=FPHI(FAMP(AAA),AAA)
    10   AAA=AAA-ACHNGE
         IF (AAA.LT.0.) GO TO 40
         F2=FPHI(FAMP(AAA),AAA)
         SINCHK=F1*F2
         IF (SINCHK.LT.0.) GO TO 20
    15   J=0
         F1=F2
         GO TO 10
    20   BBB=AAA+ACHNGE
    30   CCC=.5*(AAA+BBB)
         J=J+1
         IF (J.GT.500) GO TO 15
         FCHK=FPHI(FAMP(CCC),CCC)
         QUIT=.0000001
         IF (ABS(FCHK).LE.QUIT) GO TO 40
         SINCHK=F1*FCHK
         IF (SINCHK.LT.0.) AAA=CCC
         IF (SINCHK.GT.0.) BBB=CCC
         GO TO 30
    40   PHI=CCC
```

```
      AMP=FAMP(CCC)
      TAU=0.
      DELTA=COS(ATAN((2.*B*OMEGA)/(OMEGA**2.-OMEGA0**2.)))
      R=.04/OMEGA
 **** LOOP TO FIND XOFTAU ****************************************

      DO 200 M=1,2
        XOFTAU(M)=AMP*COS(OMEGA*TAU+PHI)+.5*(COS(2.*OMEGA*TAU-
     /    PHI)/(-1.*DEN)-COS(PHI)/OMEGA0**2.)*XI*AMP+.5*((
     /    ALPHA1-1.5*OMEGA**2.)/OMEGA0**2.-(ALPHA1+1.5*OMEGA**2.
          )/(-1.*
     /    DEN)*COS(2.*OMEGA*TAU+2.*PHI))*AMP**2.
        TAU=TAU+R
200   CONTINUE
      XMAX=XOFTAU(1)
***** LOOP TO FIND THE MAXIMUM VALUE OF XOFTAU ****************

      DO 300 N=1,2
       IF (XMAX.LT.XOFTAU(N)) XMAX=XOFTAU(N)
300   CONTINUE
      XMAX=XMAX*DELTA
       COSPH=COS(PHI)
       XMAX=AMP*COSPH
     RETURN
     END
```

February 1983

REPORTS DISTRIBUTION LIST FOR ONR PHYSICS DIVISION OFFICE
UNCLASSIFIED CONTRACTS

Director Defense Advanced Research Projects Agency Attn: Technical Library 1400 Wilson Blvd. Arlington, Virginia 22209	3 copies
Office of Naval Research Physics Division Office (Code 412) 800 North Quincy Street Arlington, Virginia 22217	3 copies
Office of Naval Research Director, Technology (Code 200) 800 North Quincy Street Arlington, Virginia 22217	1 copy
Naval Research Laboratory Department of the Navy Attn: Technical Library Washington, DC 20375	3 copies
Office of the Director of Defense Research and Engineering Information Office Library Branch The Pentagon Washington, DC 20301	3 copies
U.S. Army Research Office Box 1211 Research Triangle Park North Carolina 27709	2 copies
Defense Technical Information Center Cameron Station Alexandria, Virginia 22314	12 copies
Director, National Bureau of Standards Attn: Technical Library Washington, DC 20234	1 copy
Commanding Officer Office of Naval Research Western Detachment Office 1030 East Green Street Pasadena, California 91101	3 copies
Commanding Officer Office of Naval Research Eastern/Central Detachment Office 495 Summer Street Boston, Massachusetts 02210	3 copies

Commandant of the Marine Corps
Scientific Advisor (Code RD-1)
Washington, DC 20380 — 1 copy

Naval Ordnance Station
Technical Library
Indian Head, Maryland 20640 — 1 copy

Naval Postgraduate School
Technical Library (Code 0212)
Monterey, California 93940 — 1 copy

Naval Missile Center
Technical Library (Code 5632.2)
Point Mugu, California 93010 — 1 copy

Naval Ordnance Station
Technical Library
Louisville, Kentucky 40214 — 1 copy

Commanding Officer
Naval Ocean Research & Development Activity
Technical Library
NSTL Station, Mississippi 39529 — 1 copy

Naval Explosive Ordnance Disposal Facility
Technical Library
Indian Head, Maryland 20640 — 1 copy

Naval Ocean Systems Center
Technical Library
San Diego, California 92152 — 1 copy

Naval Surface Weapons Center
Technical Library
Silver Spring, Maryland 20910 — 1 copy

Naval Ship Research and Development Center
Central Library (Code L42 and L43)
Bethesda, Maryland 20084 — 1 copy

Naval Avionics Facility
Technical Library
Indianapolis, Indiana 46218 — 1 copy

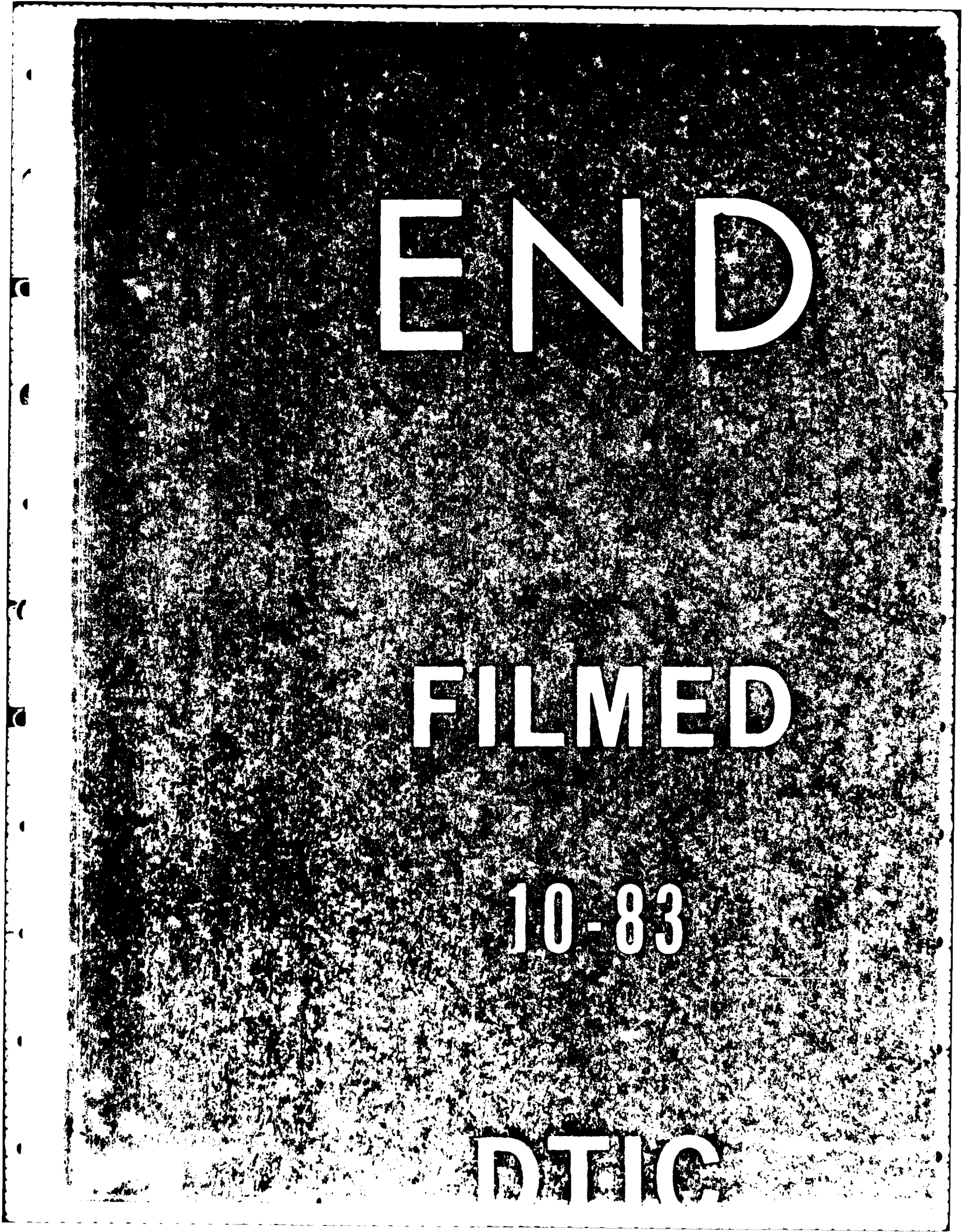
END
FILMED
10-83
DTIC